

Tomographical application of CAFADIS plenoptic sensor

Speaker: Juan M. Trujillo Sevilla
University of La Laguna, Spain

Edinburgh, 25 march 2014



Index

i. Description of the plenoptic sensor

- Basic plenoptic sensor
- Bibliography
- Lightfield
- CAFADIS camera

ii. Non astronomy applications

- Multiview. 3D stereo
- Refocus
- Depth maps
- Microscopy

iii. Astronomy applications

- Wavefront sensing
- Wavefront tomography
- LGS profile measurement
- Image deconvolution



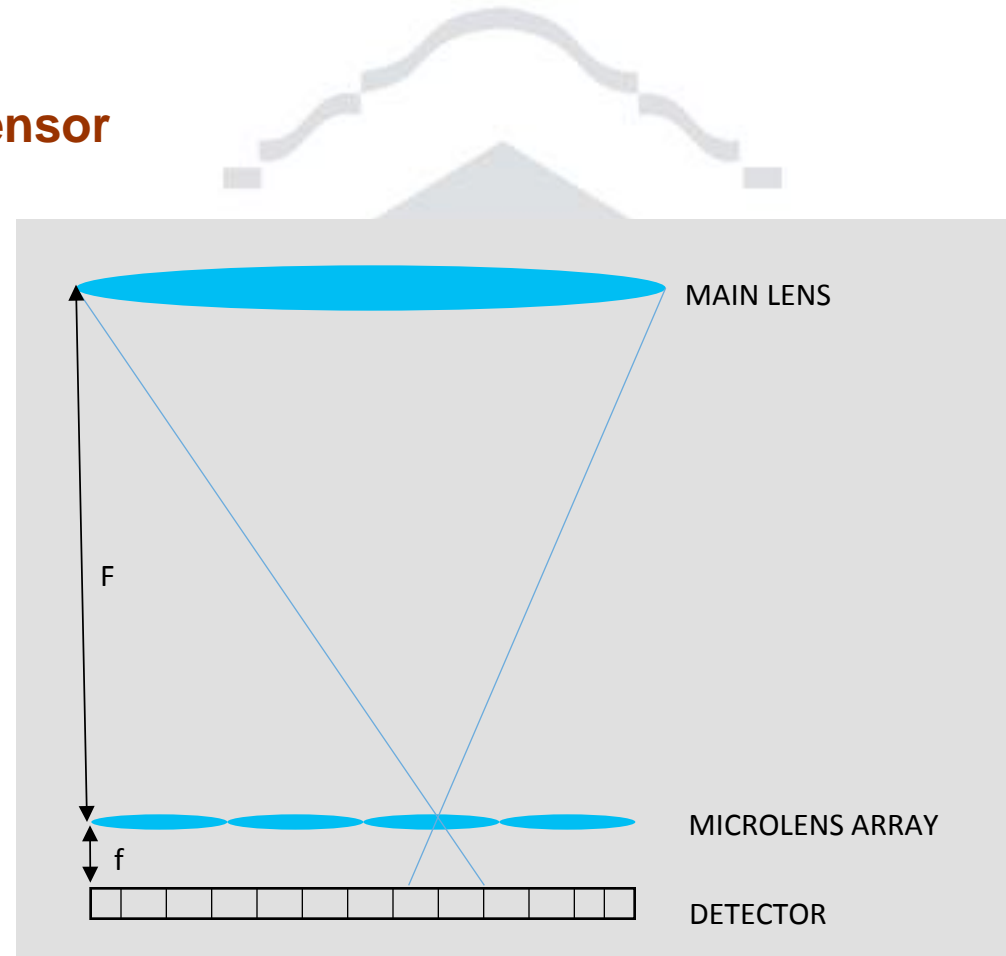
i. Description of the plenoptic sensor

- Basic plenoptic sensor

Micro lens array placed in the main lens focal plane.

Detector placed at the focal plane of the micro lens array.

The micro lens focal distance is on the order of hundreds of microns.



i. Description of the plenoptic sensor

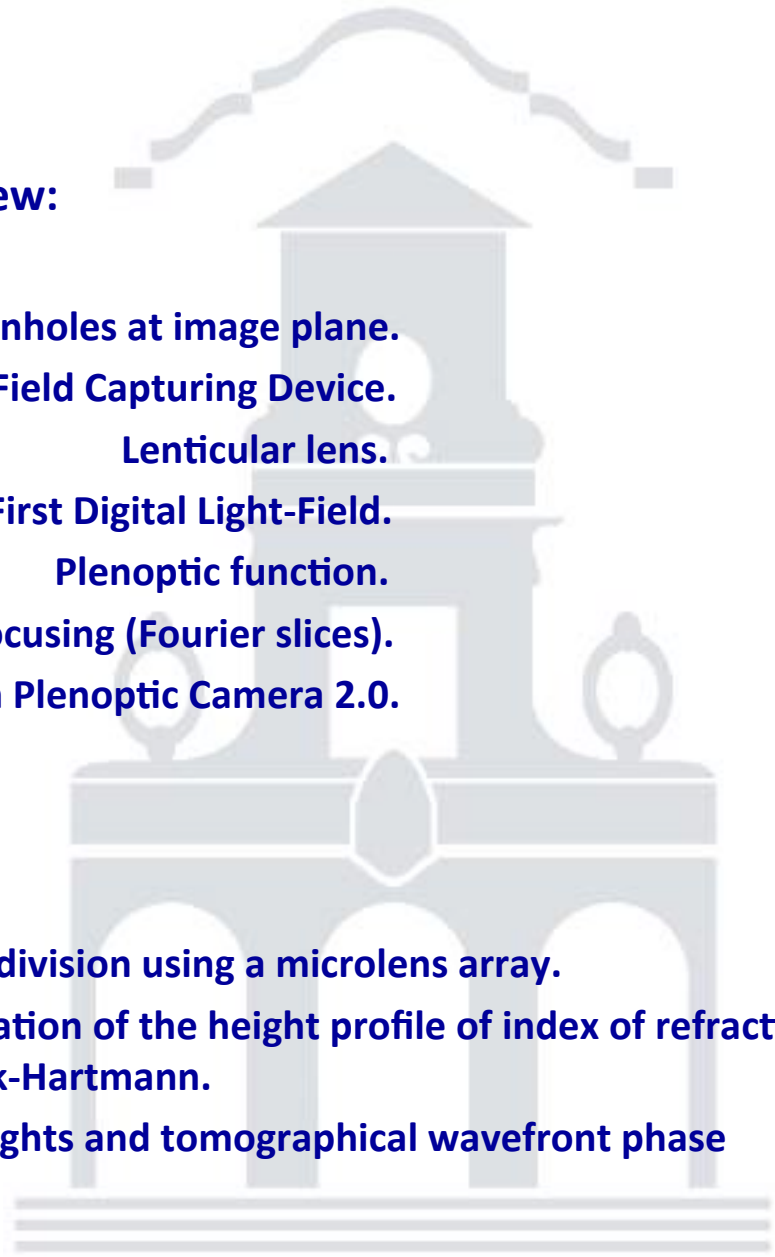
• Bibliography

From the computer vision point of view:

- Ives F. (1903): Array of pinholes at image plane.
- Lippmann (1908): First Described Light-Field Capturing Device.
- Ives H. (1930): Lenticular lens.
- Chutjian (1968): First Digital Light-Field.
- Adelson and Wang (1992): Plenoptic function.
- Ng R. et al (2005): Refocusing (Fourier slices).
- Georgiev (2009): Superresolution with Plenoptic Camera 2.0.

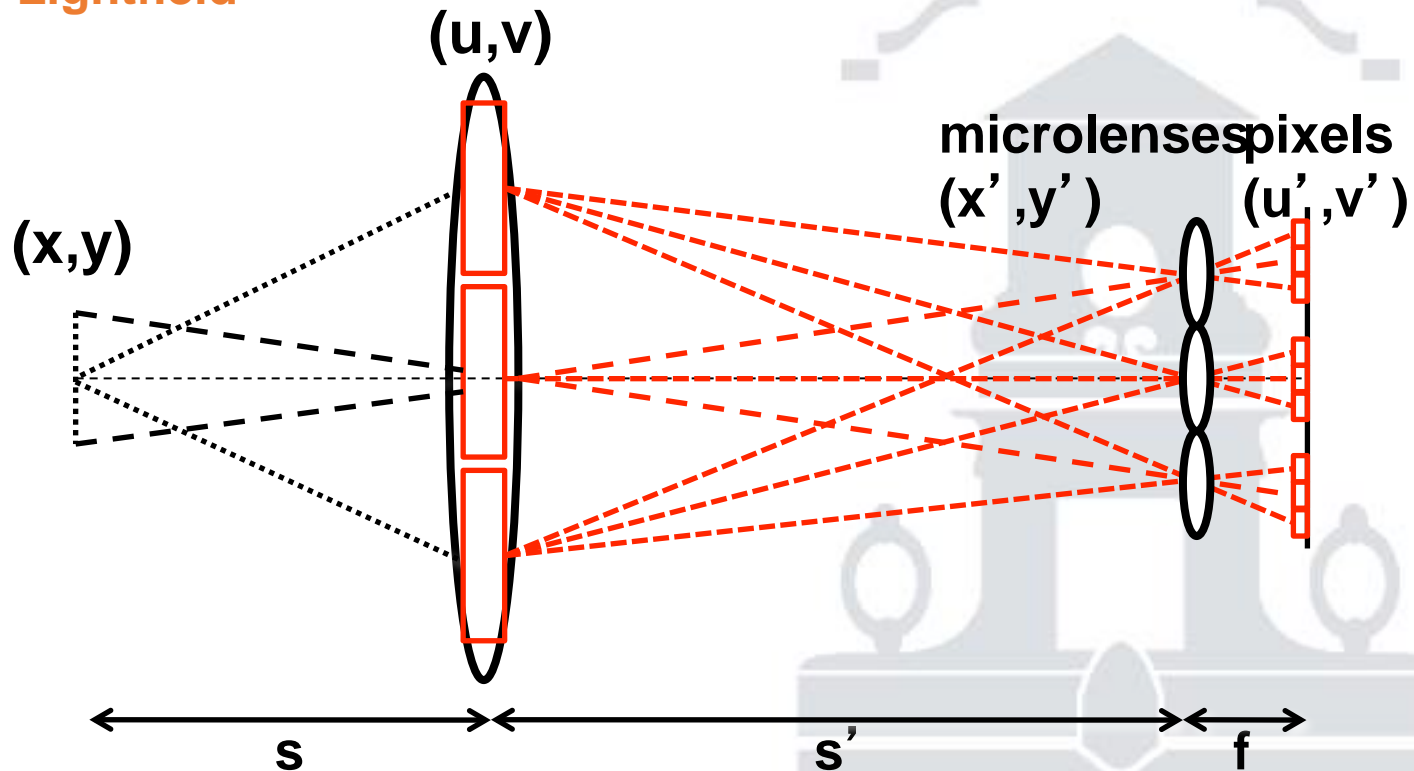
From the wave optics point of view:

- Clare and Lane (2005). Focal plane subdivision using a microlens array.
- T.A. Wadmann et al. (2007). Determination of the height profile of index of refraction fluctuations using wide field of view Shack-Hartmann.
- Rodriguez-Ramos et al. (2008). LGS heights and tomographical wavefront phase distribution using the plenoptic sensors.



i. Description of the plenoptic sensor

- Lightfield

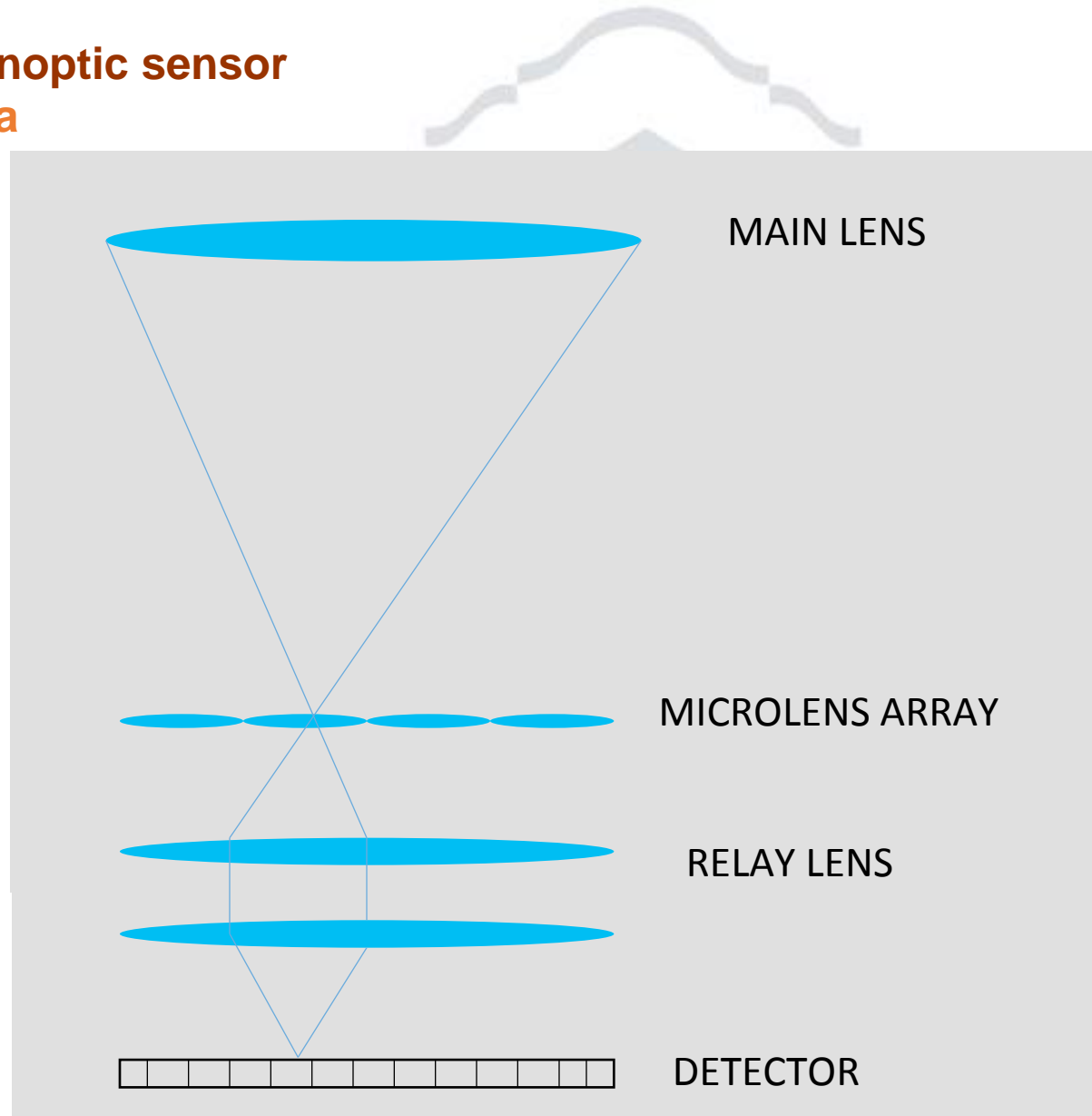


- The plenoptic camera captures the Light Field, a four-variable (x, y, u, v) volume representation of all rays and their directions.
- The microlenses sample the spatial coordinates (x, y) and the pixels sample the angular coordinates (u, v) .

i. Description of the plenoptic sensor

• CAFADIS camera

- The CAFADIS camera is a sensor patented by Universidad de La Laguna (Canary Islands, Spain).
- International patents:
PCT/ES2007/000046
PCT/ES2009/000031
- It can measure out **wavefront phases tomographically** and **scene depths** at the same time.



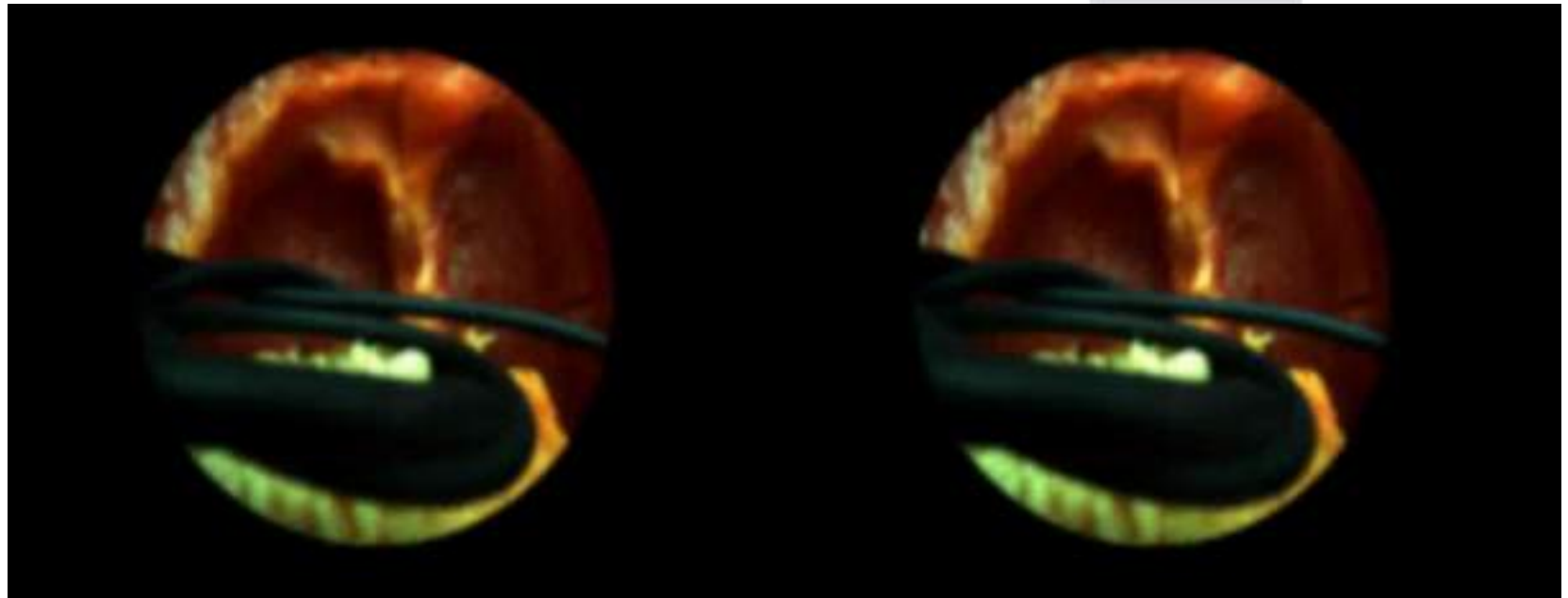
We use conventional cameras as
plenoptic cameras:



Underwater 3D imaging



Plenoptic endoscopy. Real-time 3D stereo video



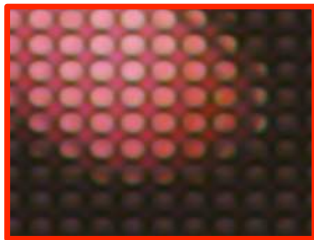
ii. Non astronomy applications

- **Multiview. 3D stereo**
- **Refocus**
- **Depth maps**
- **Microscopy**
 - **3D volume reconstruction**
 - **Refraction index tomography**

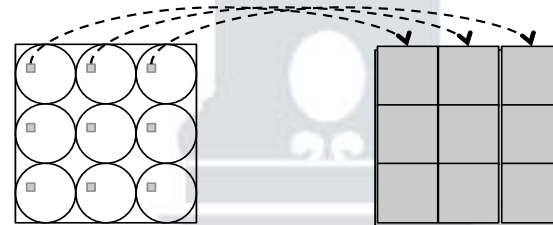


- **Multiview stereo system.** As many points of view like as pixels behind each microlens

Plenoptic Frame

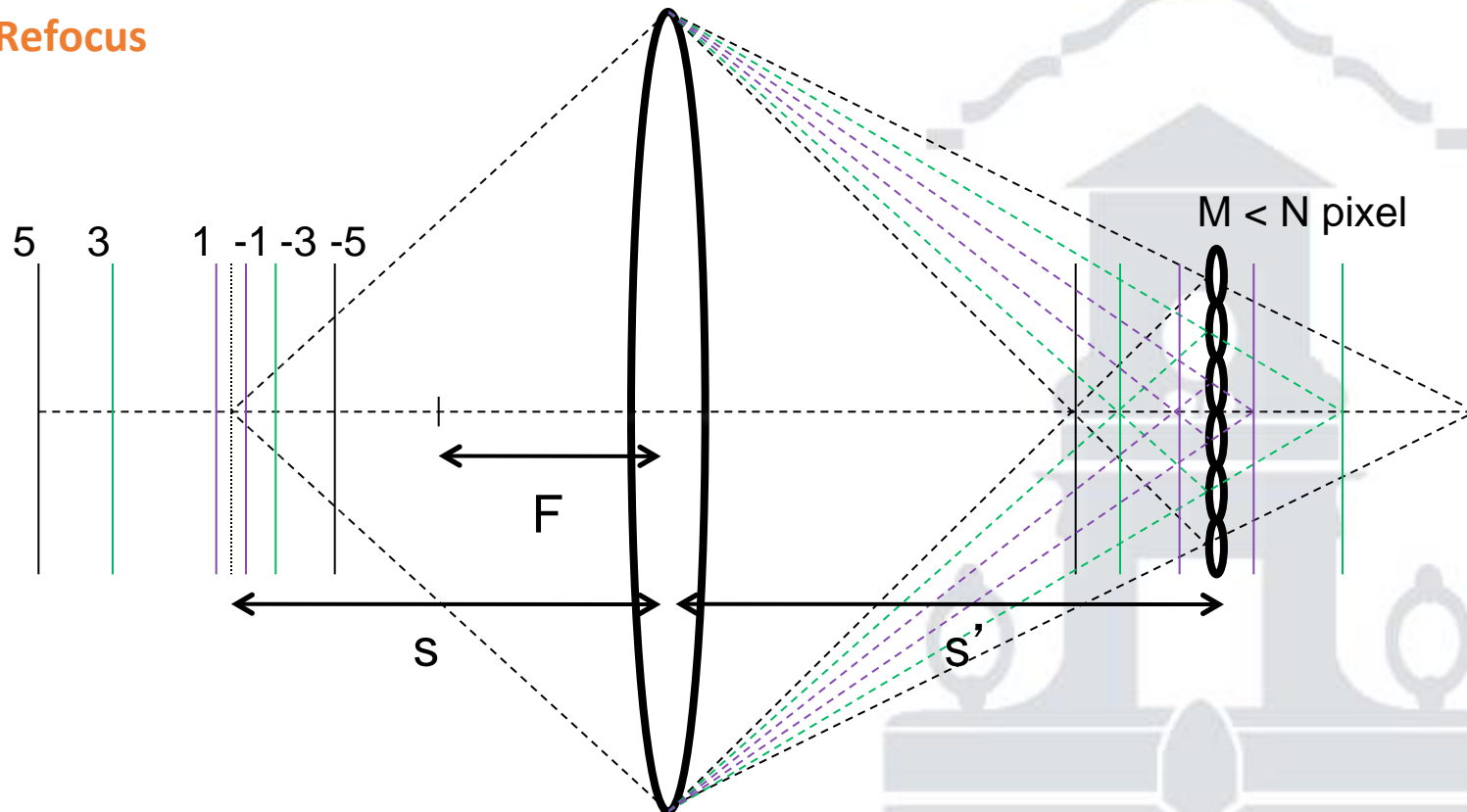


Magnified section



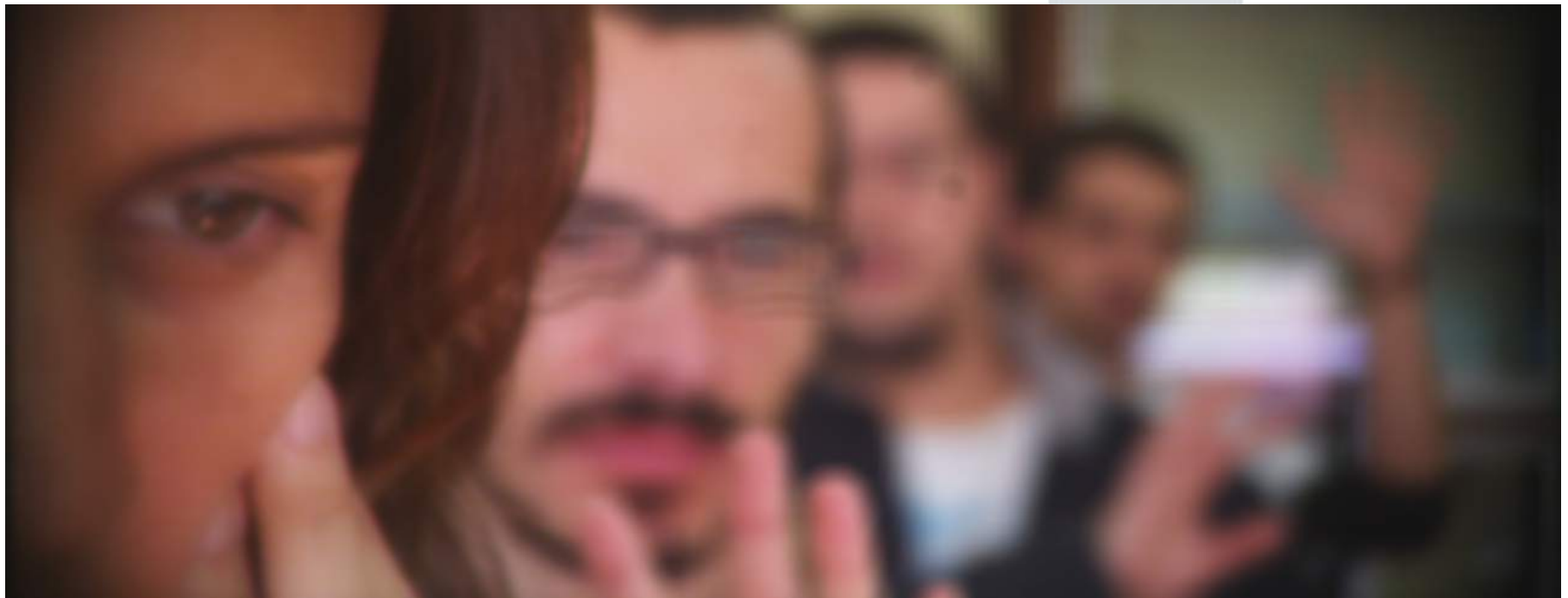
Integral image.

- Refocus



- Depending on how the pixels are combined, we retrieve the focused image of the object placed at one distance or another.
- There are different algorithms that refocus more or less planes at different distances.

- **Focal stack:**
Refocused images at different distances



- **All-in-focus and depth map**

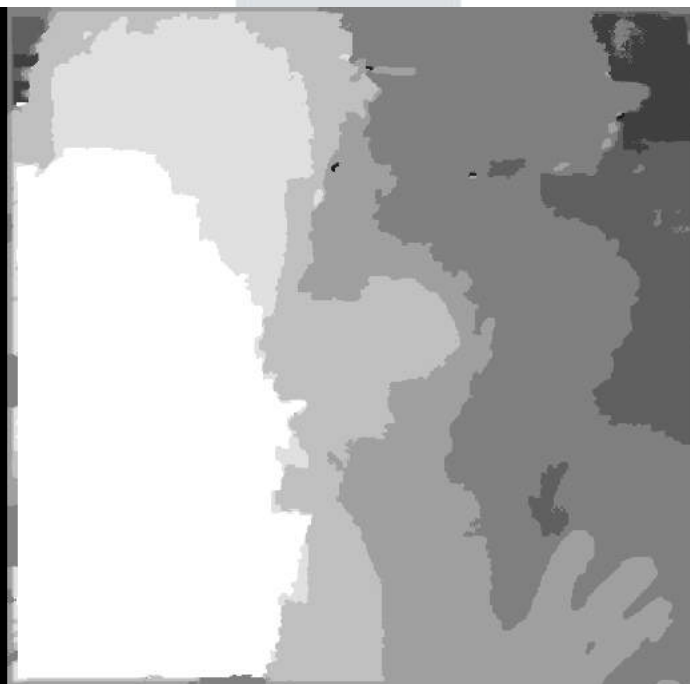


Image from: <http://graphics.stanford.edu/>

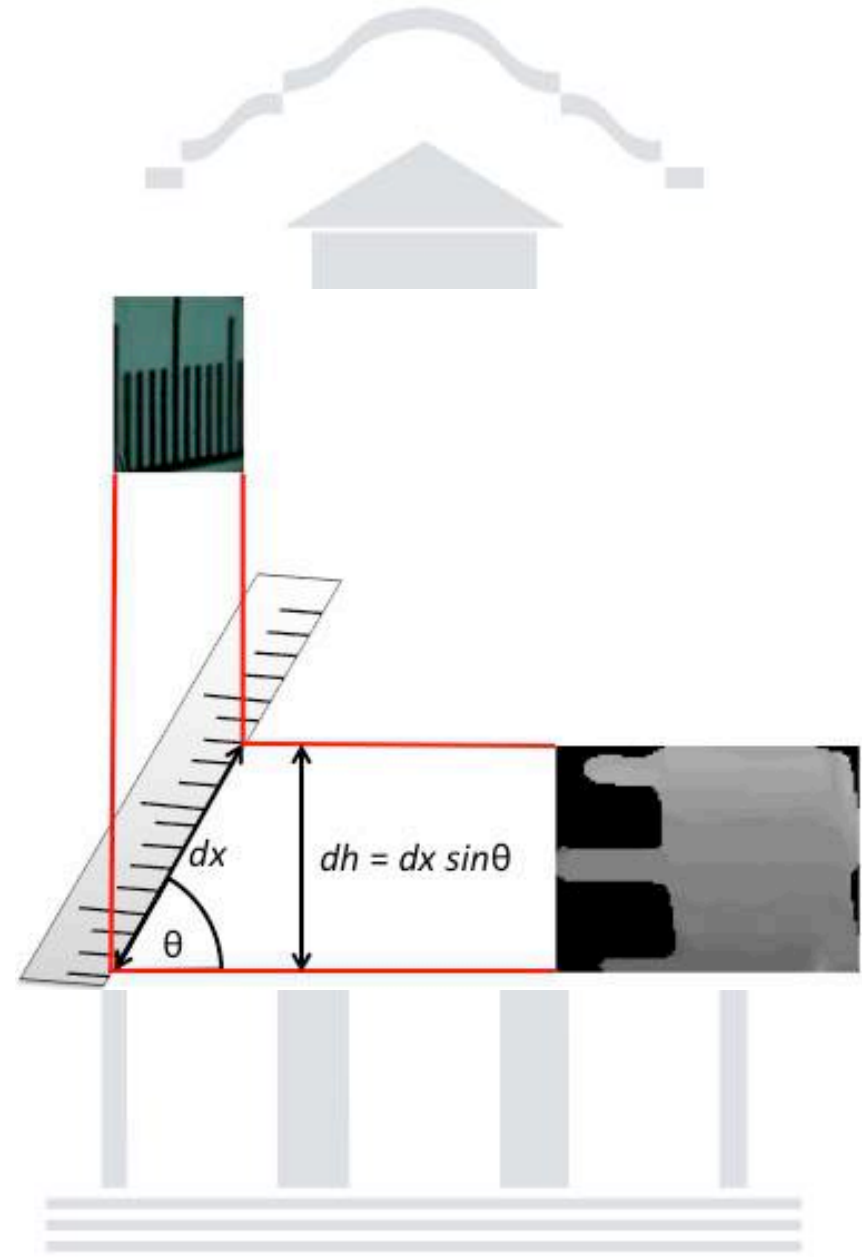
- **Plenoptic microscopy**
- **Leica M205 A Stereomicroscope with a mounted plenoptic camera**
- **Focal stacks and depth maps are possible.**
- **3D volume reconstruction of samples**



- **Depth calibration**

- In order to make accurate volume reconstructions.
- Determination of planes distribution experimentally.
- Plenoptic images of an **inclined ruler** were used.
- The lines of the ruler were used as **reference** for the depth maps.

The magnification range used was 10x-45x.



- Reference depth maps for different magnifications.
- Better results at 25x:
 - ✓ More refocused planes in FoV.
 - ✓ Less artifacts



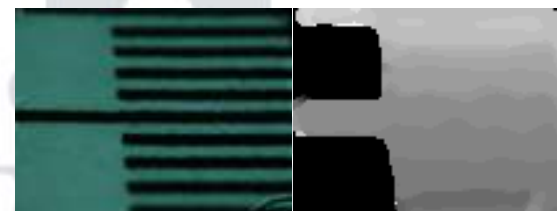
10.0X



15.0X



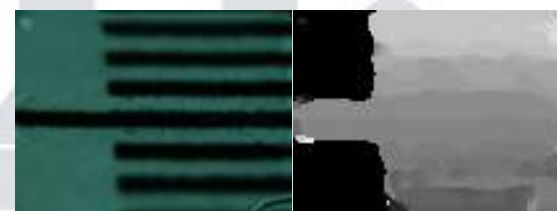
20.0X



25.0X



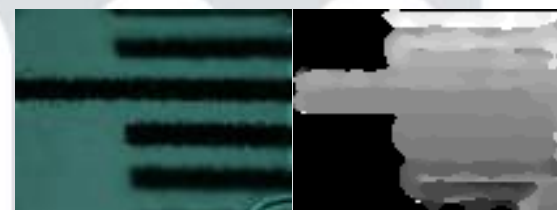
30.0X



35.0X

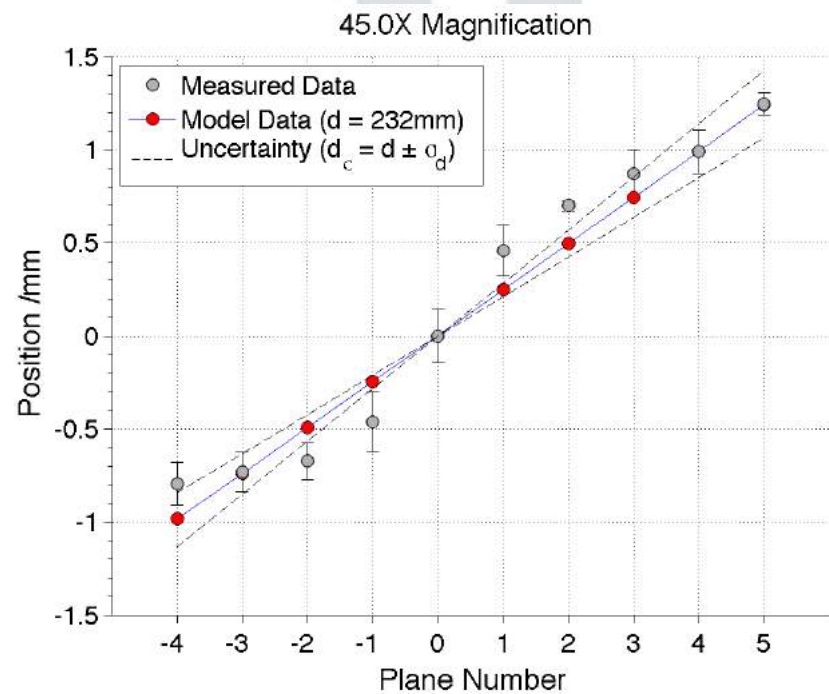
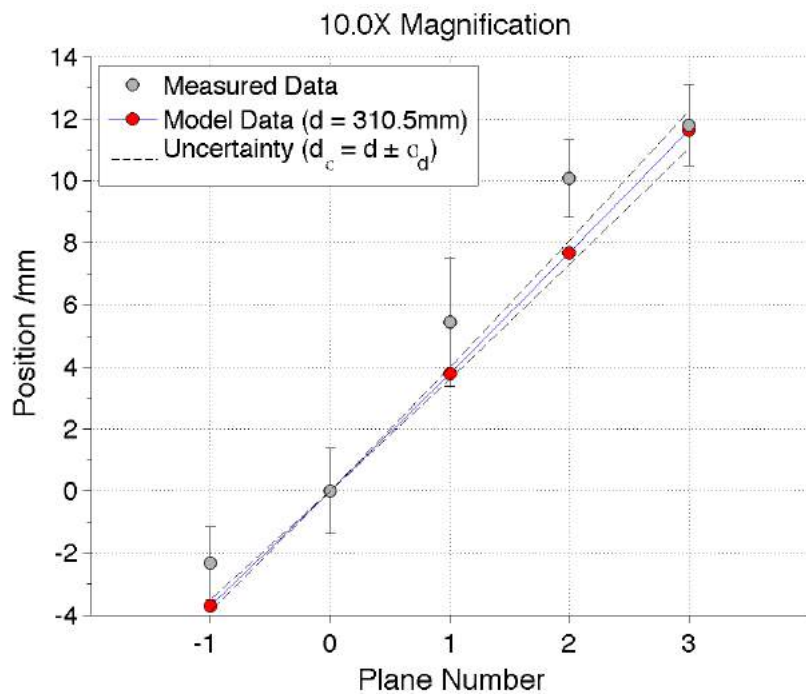


40.0X



45.0X

- Model of plane distribution based on **geometry and optical properties of microlenses**.
- Calculated plane positions follow a linear distribution.
- Estimated results are within the experimental error of the measured results.



- **Focal stack**

Focal stack:



Depth Map:



Conjugated plane:



All-in-focus:

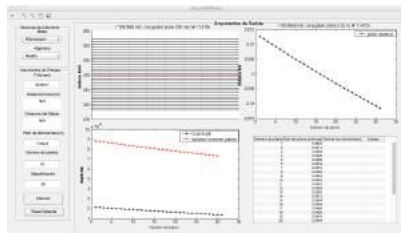


Extended depth of field

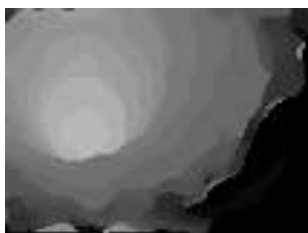
- Volume reconstruction



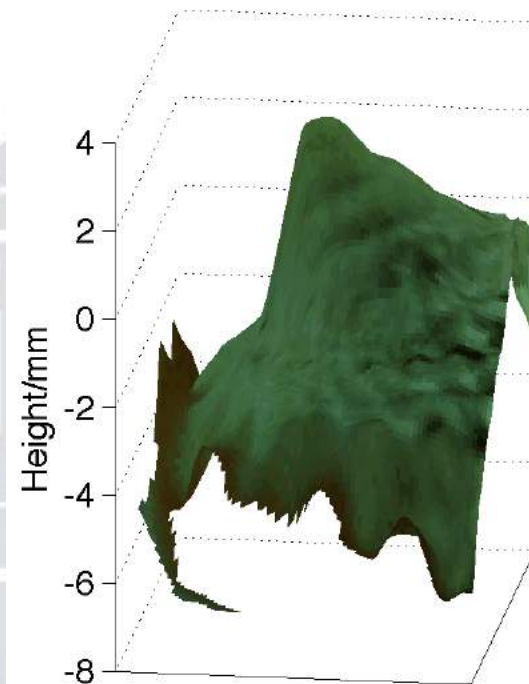
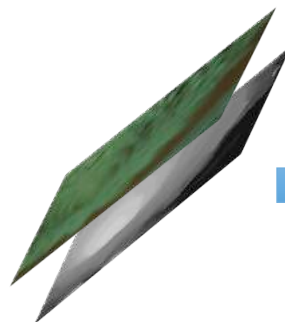
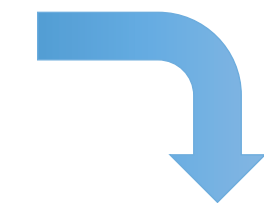
Focus plane image



Depth estimation



Depth map



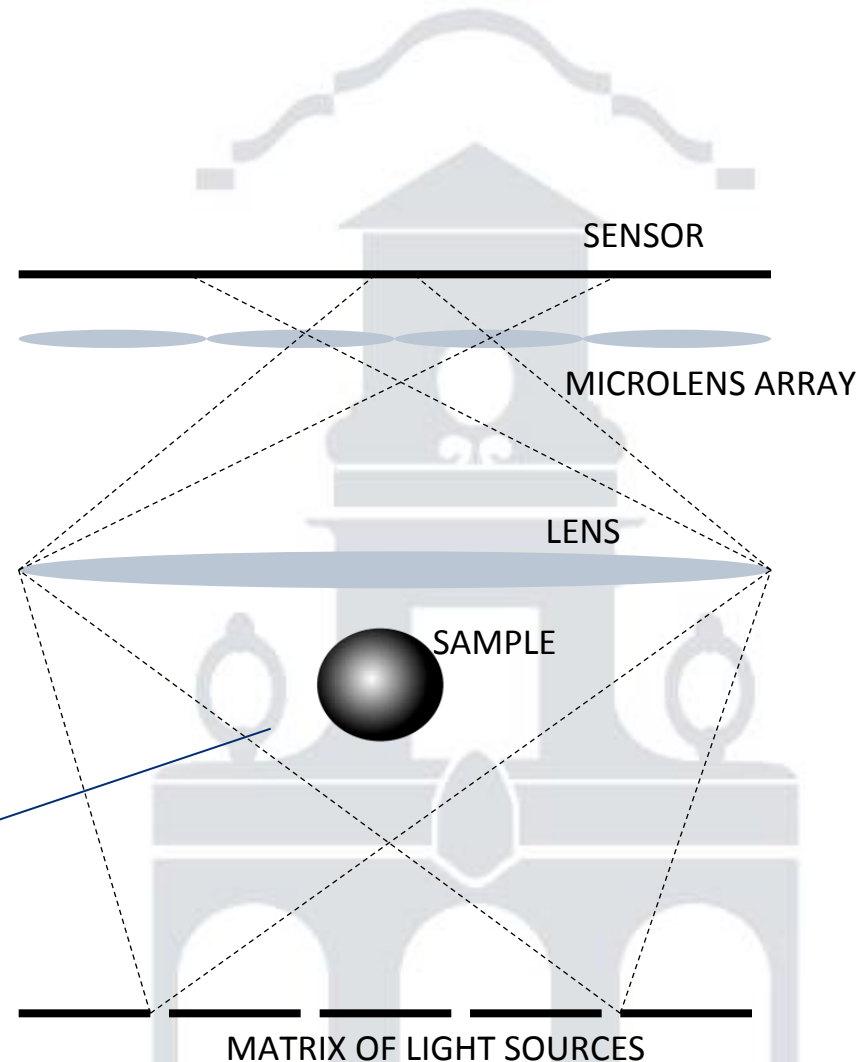
3D Volume

- **Tomographic microscopy**

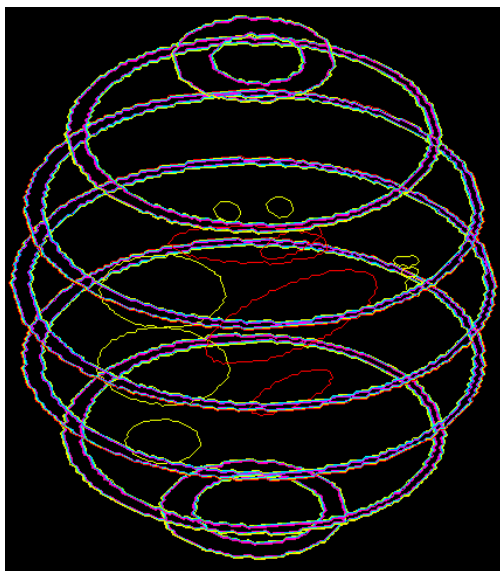
- Tomography of refraction index variations.
- Analog technique to atmospheric tomography
- No need of fixing or staining.
- Limited Field of view.
- Big number of projections needed

Shepp-Logan 3D-Phantom

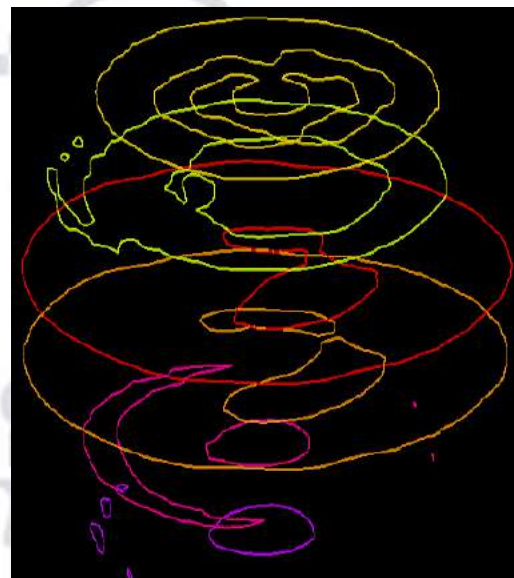
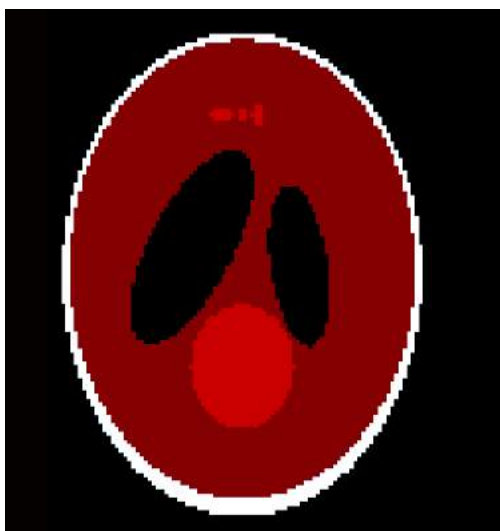
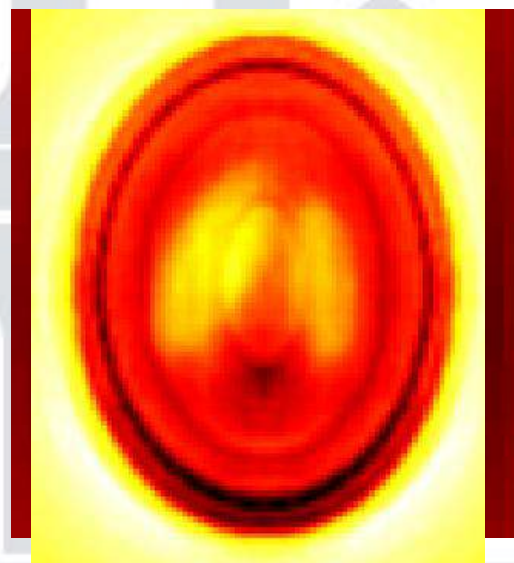
- 32x32 microlens array
- 64x64 pixels/microlens
- 16x16 point source matrix



Original volume



Restored volume

Central slice of the
original volumeCentral slice of
restored volume

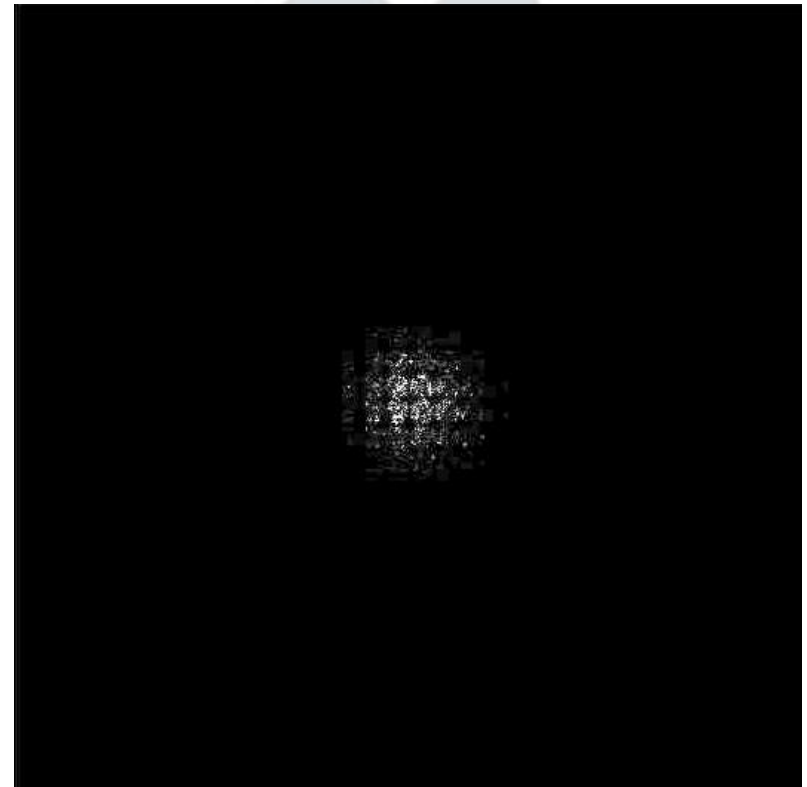
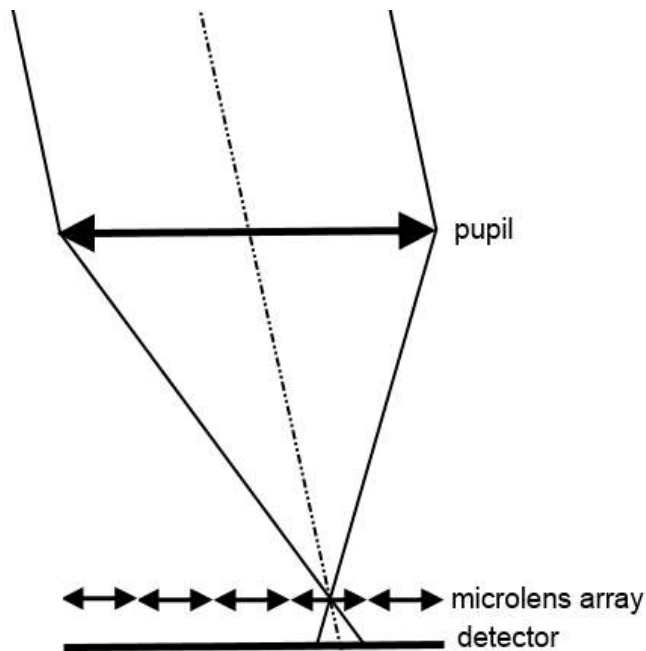
iii. Astronomy applications

- Wavefront sensing
- Wavefront tomography
- LGS profile measurement
- Image deconvolution

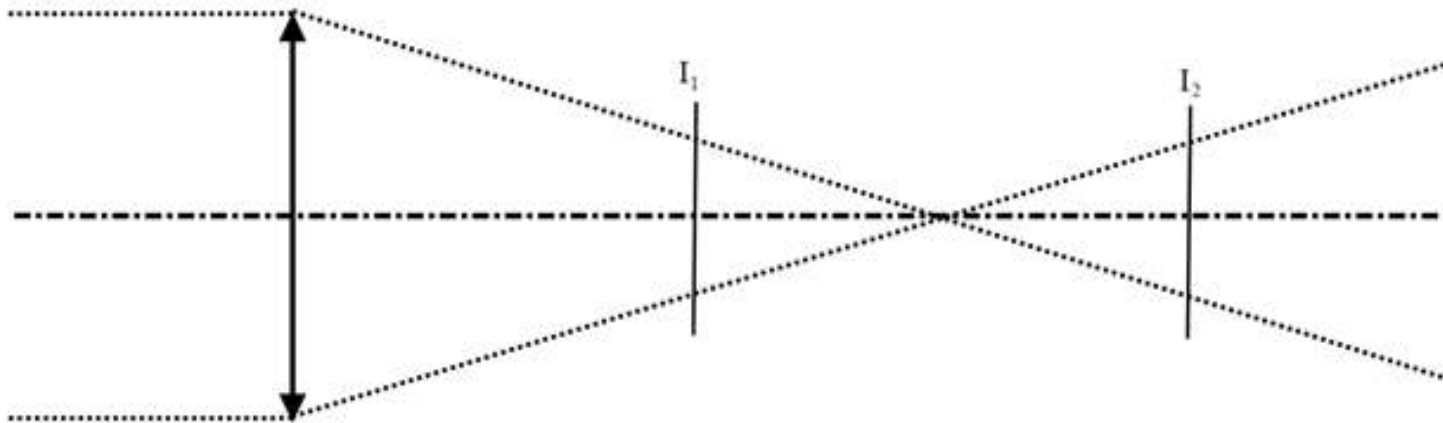


- **Wavefront sensing**

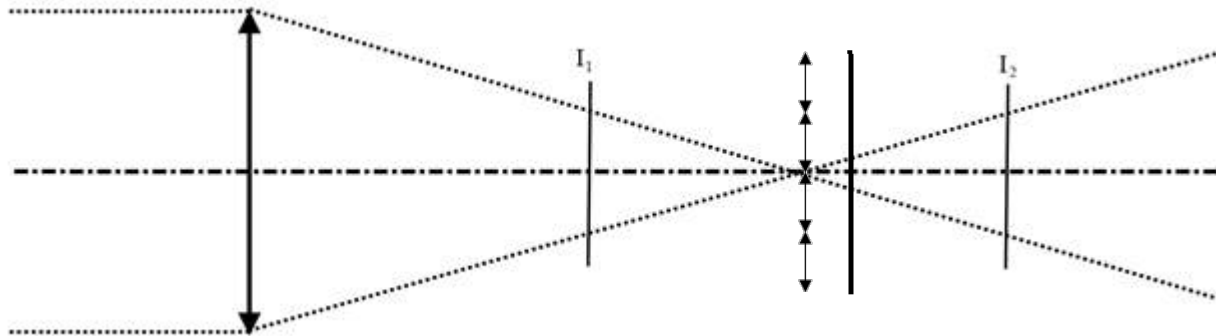
- Three different wavefront sensors can be derived from the plenoptic sensor:
 1. Curvature sensor
 2. Shack-Hartmann sensor
 3. Pyramid sensor



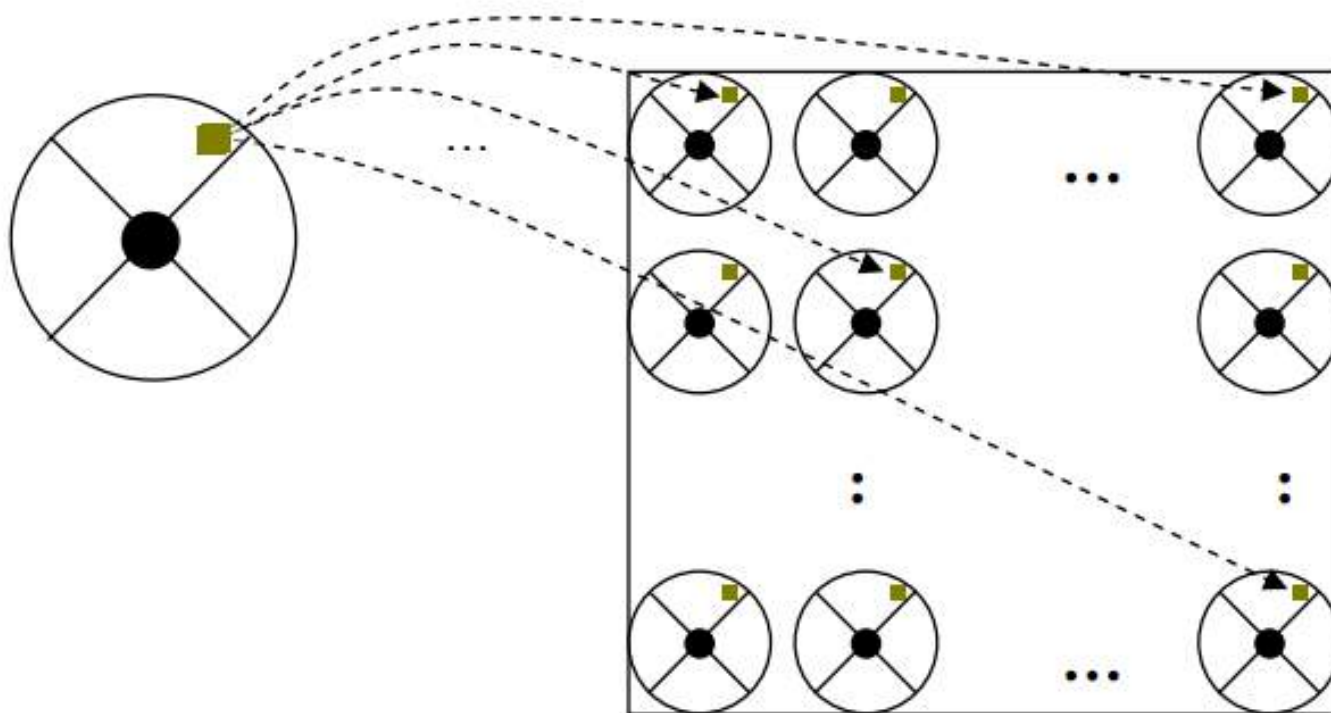
- Curvature sensor from plenoptic sensor
- Wavefront sensing from **two symmetrical out of focus images**.
- Out of focus images could be obtained by **refocusing two symmetric planes**.



- Curvature sensor from plenoptic sensor



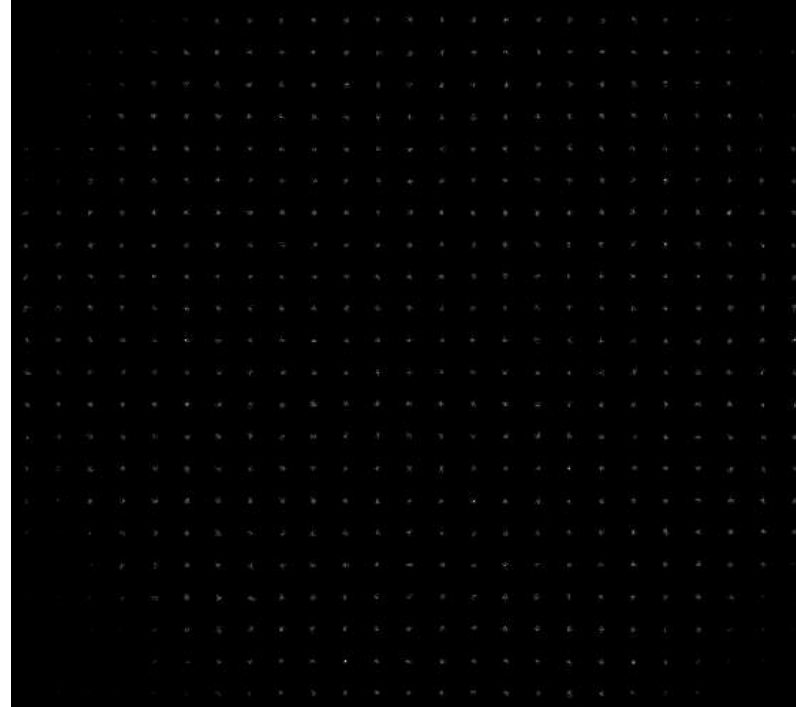
- **Shack-Hartmann sensor from plenoptic sensor**
 - **Reordering pixels**, every pupil coordinate is re-imaged on the corresponding position of each microlens, depending on the arriving angle of the incoming ray .
 - **Multiple views** of the object.
 - **Correspondence between pupil and pupil images.**



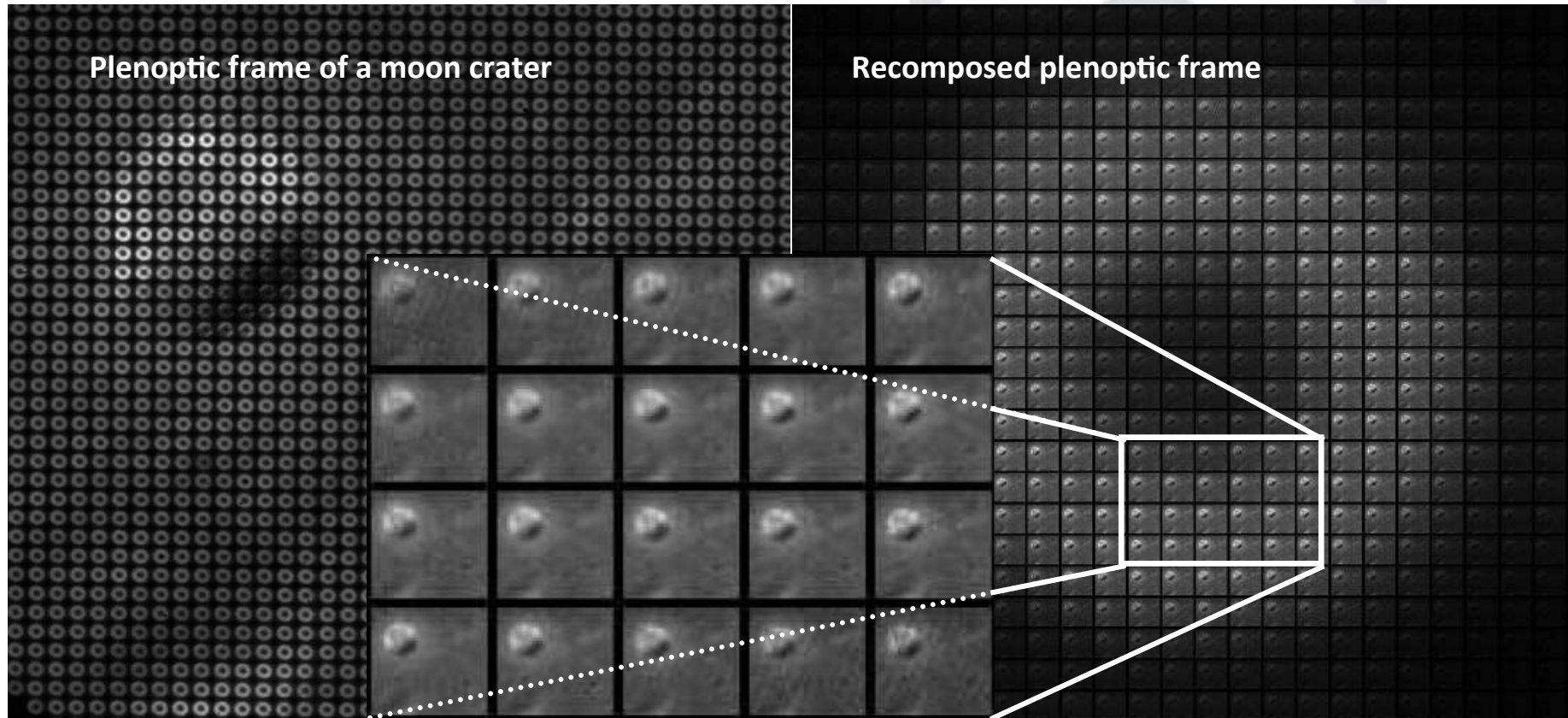
Plenoptic frame of a point source



Recomposed plenoptic frame

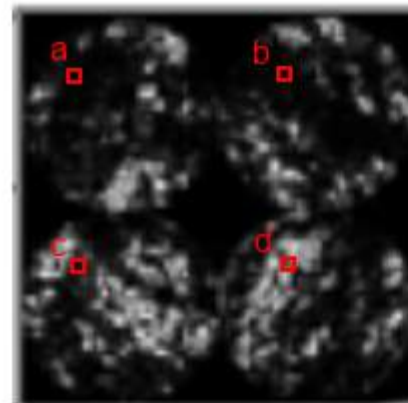
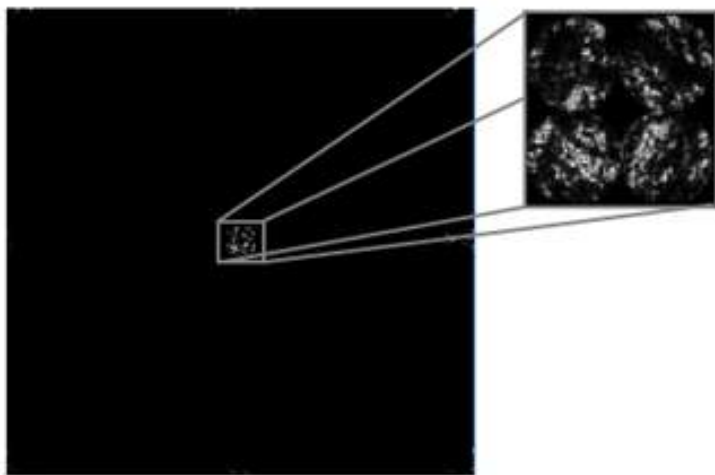
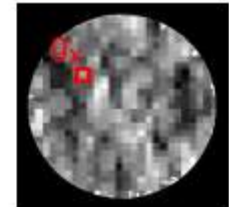
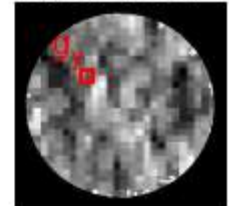


- **Plenoptic image: 32x32 microlenses of 25x25 pixels each.**
- **Recomposed image: 25x25 subimages of 32x32 pixels**



The differences between subimages are due to the differential turbulence traversed by the rays that form every subimage.

- **Pyramid sensor from plenoptic sensor**
 - Subdivision of the focal plane plenoptic sensor.
 - Plenoptic sensor can be seen as a generalization of pyramid sensor **without modulation**.

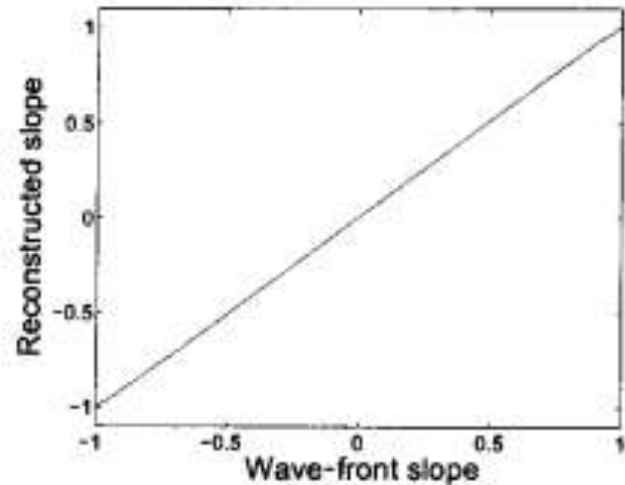
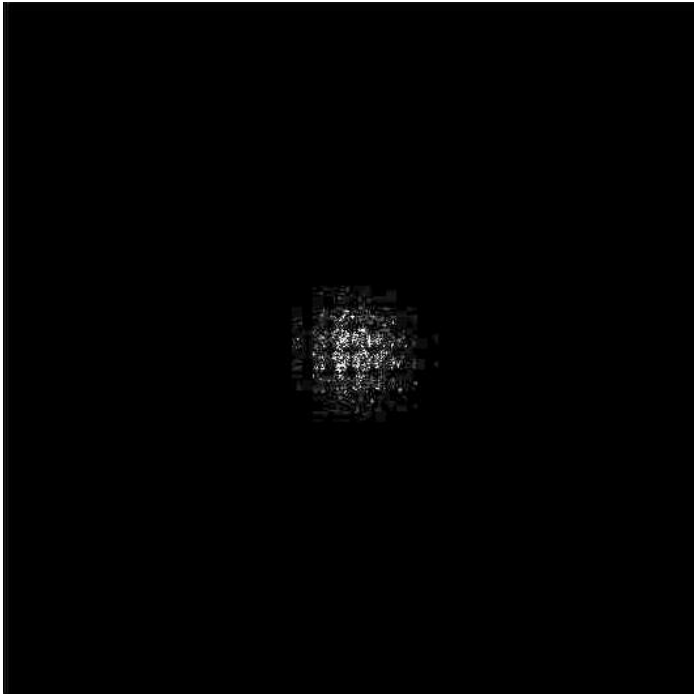
HORIZONTAL
GRADIENTSVERTICAL
GRADIENTS

t. A,

$$g_x = \frac{(a - b) + (c - d)}{a + b + c + d}$$

$$g_y = \frac{(a - c) + (b - d)}{a + b + c + d}$$

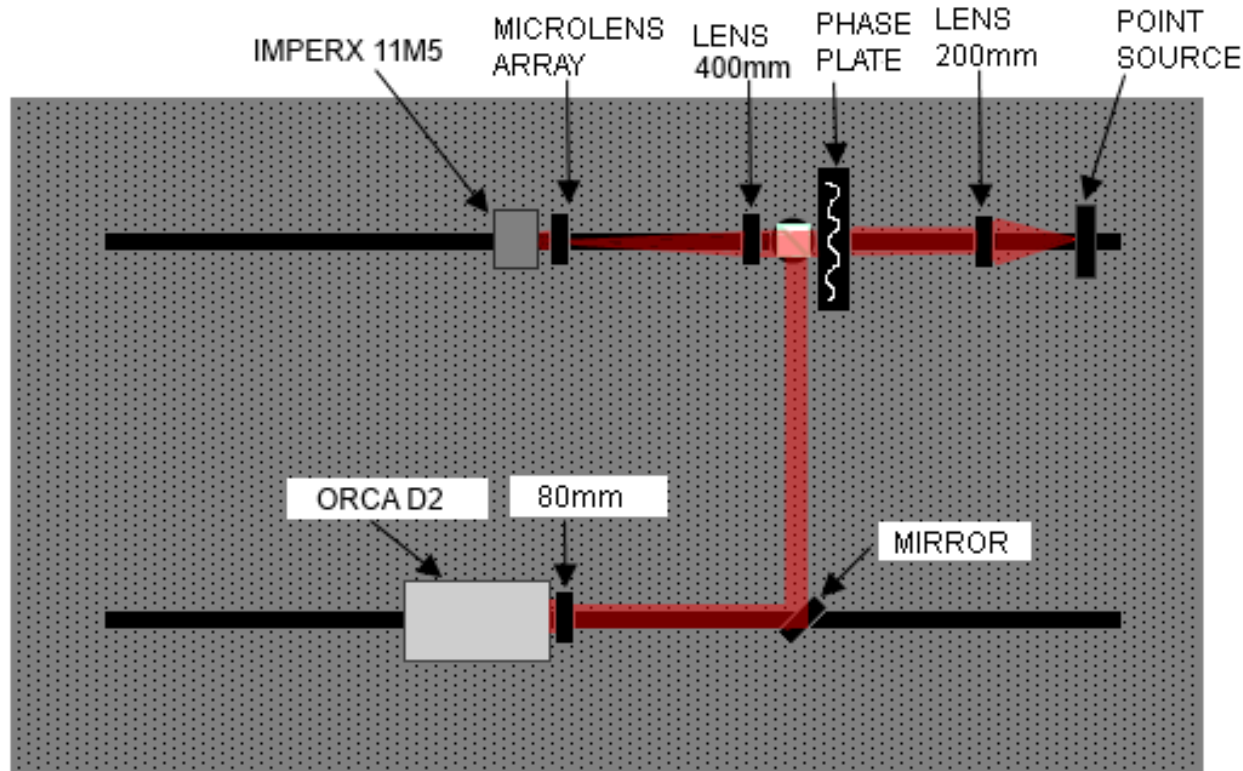
- **Pyramid sensor from plenoptic sensor**
 - Modulation is used in pyramid sensor to improve linearity.
 - No modulation is possible in the plenoptic sensor.



- **No modulation is needed since spot size is bigger than microlens diameter*.**

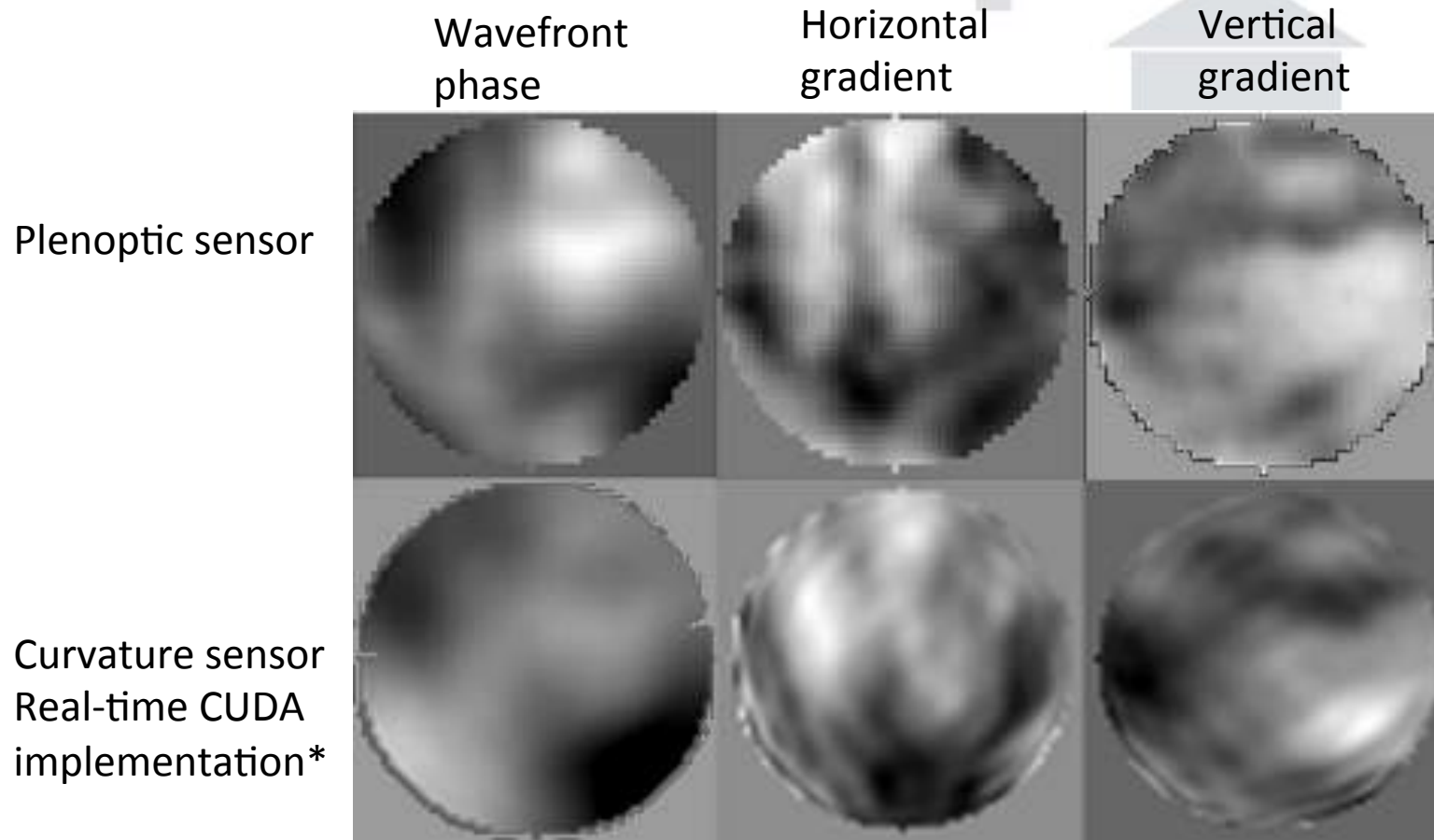
*R. M. Clare and R. G. Lane, "Wave-front sensing from subdivision of the focal plane with a lenslet array.," *Journal of the Optical Society of America. A, Optics, image science, and vision*, vol. 22, no. 1, pp. 117–25, Jan. 2005

- Laboratory tests



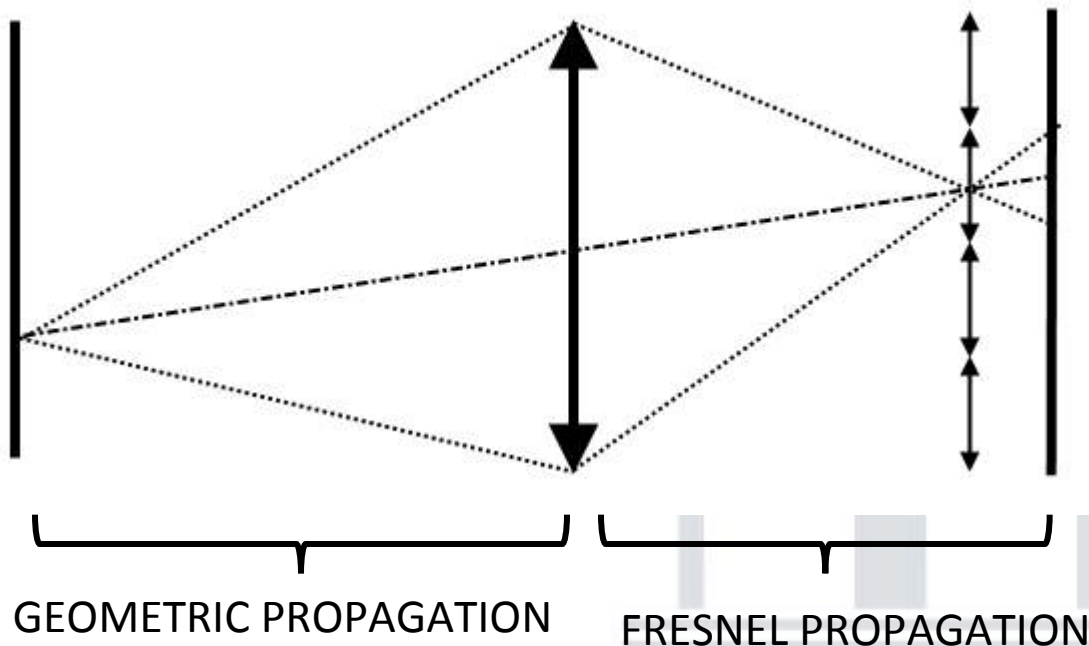
- Laboratory test to verify the plenoptic sensor performance.
- The plenoptic and the curvature sensors are working in parallel.
- 1.5mm r_0 phase plate
- Both sensors are measuring the same phase

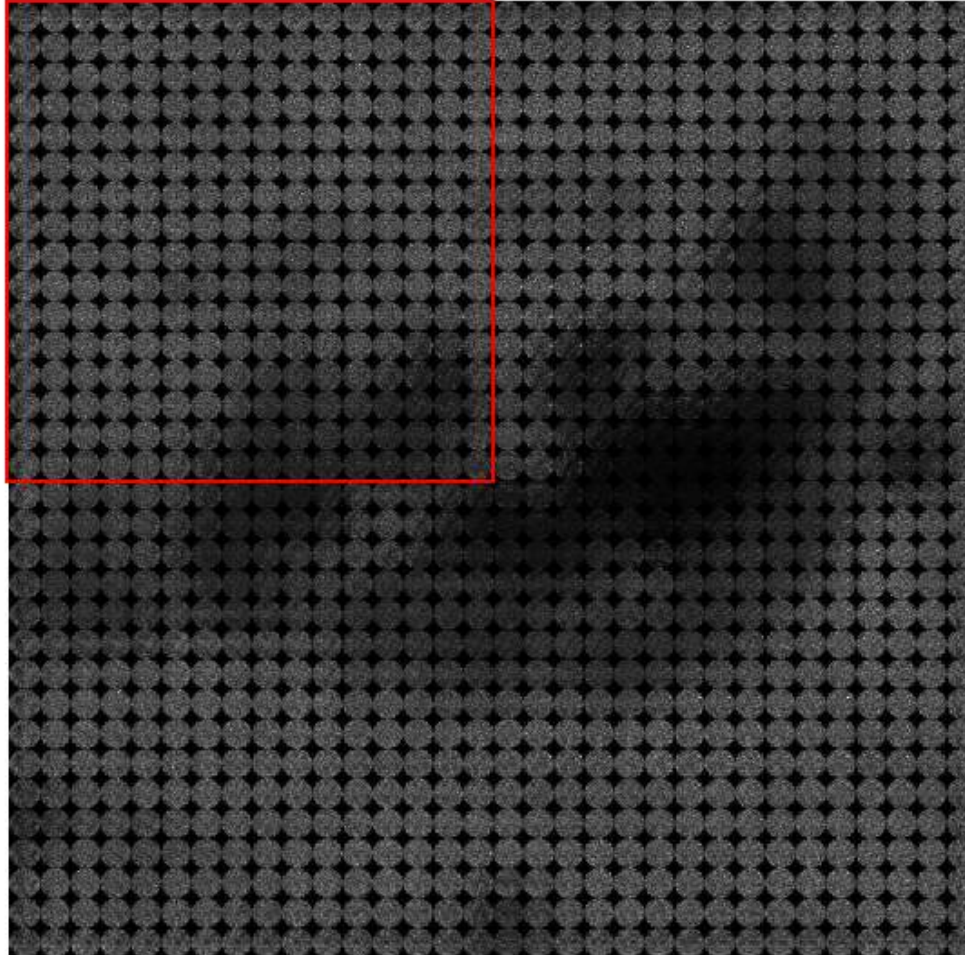
- Laboratory tests



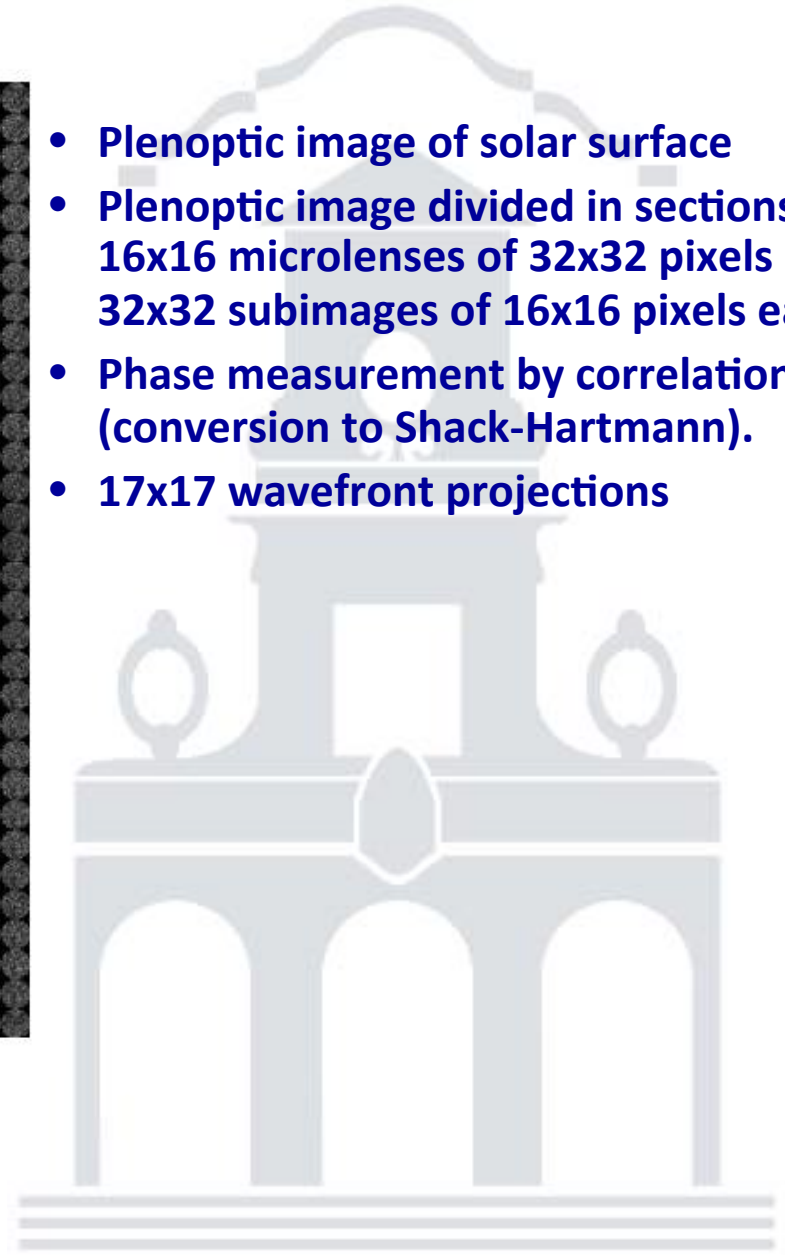
*van Dam, Marcos A., and Richard G. Lane. "Wave-front sensing from defocused images by use of wave-front slopes." *Applied optics* 41.26 (2002): 5497-5502.

- **Tomography using extended object as reference**
- Use of extended objects instead of LGS. e.g. solar telescopes.
- **Simulation:**
 - f/50 4m diameter telescope.
 - Fresnel propagation to simulate the plenoptic sensor.
 - Geometric propagation from every point of the object to the pupil.
 - 2048x2048 object resolution (2048² propagations)



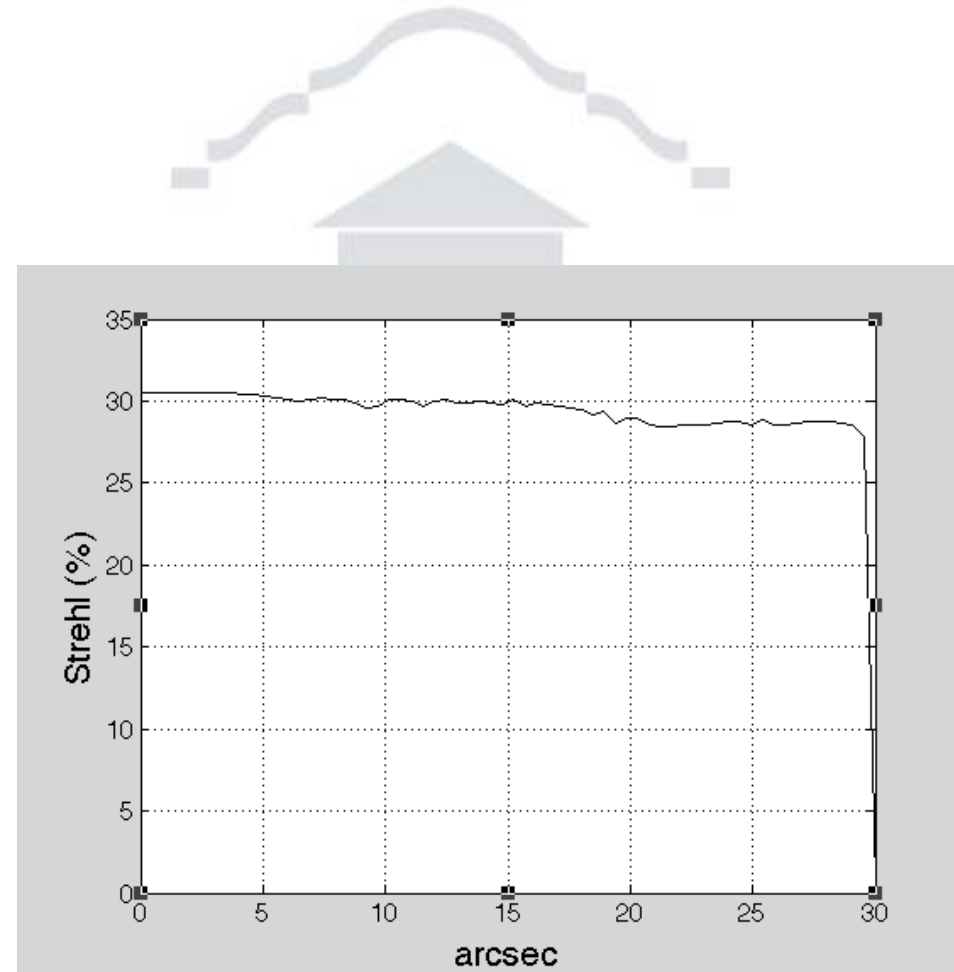
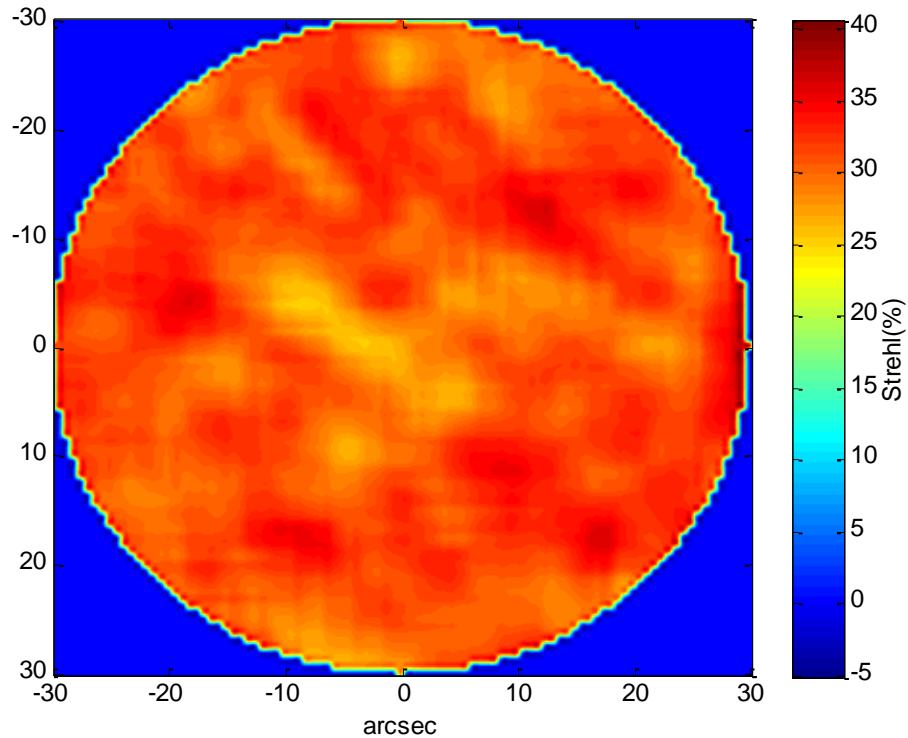


- Plenoptic image of solar surface
- Plenoptic image divided in sections of 16x16 microlenses of 32x32 pixels each -> 32x32 subimages of 16x16 pixels each.
- Phase measurement by correlations (conversion to Shack-Hartmann).
- 17x17 wavefront projections



- **Strehl map**

Correction at 0m and 1500m

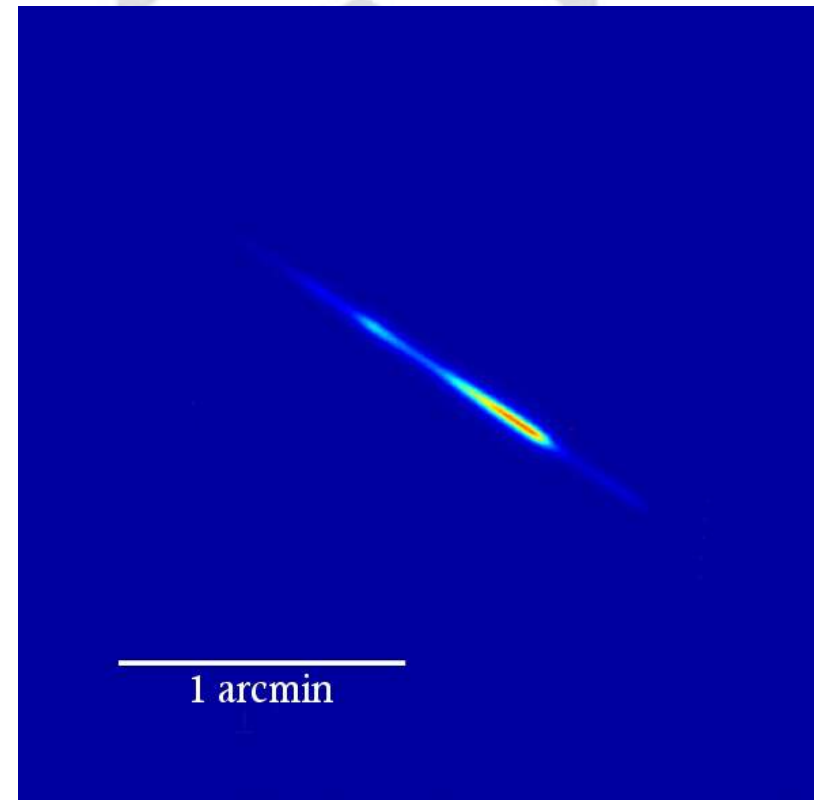


- **LGS profile measurement**

1. **Elongated source of light.**
2. **Sporadic bright layers**
3. **Variations in the height**

- 3D distribution of LGS is required to measure the wavefront properly.

- The 3D distribution of the LGS can be measured with a plenoptic sensor.

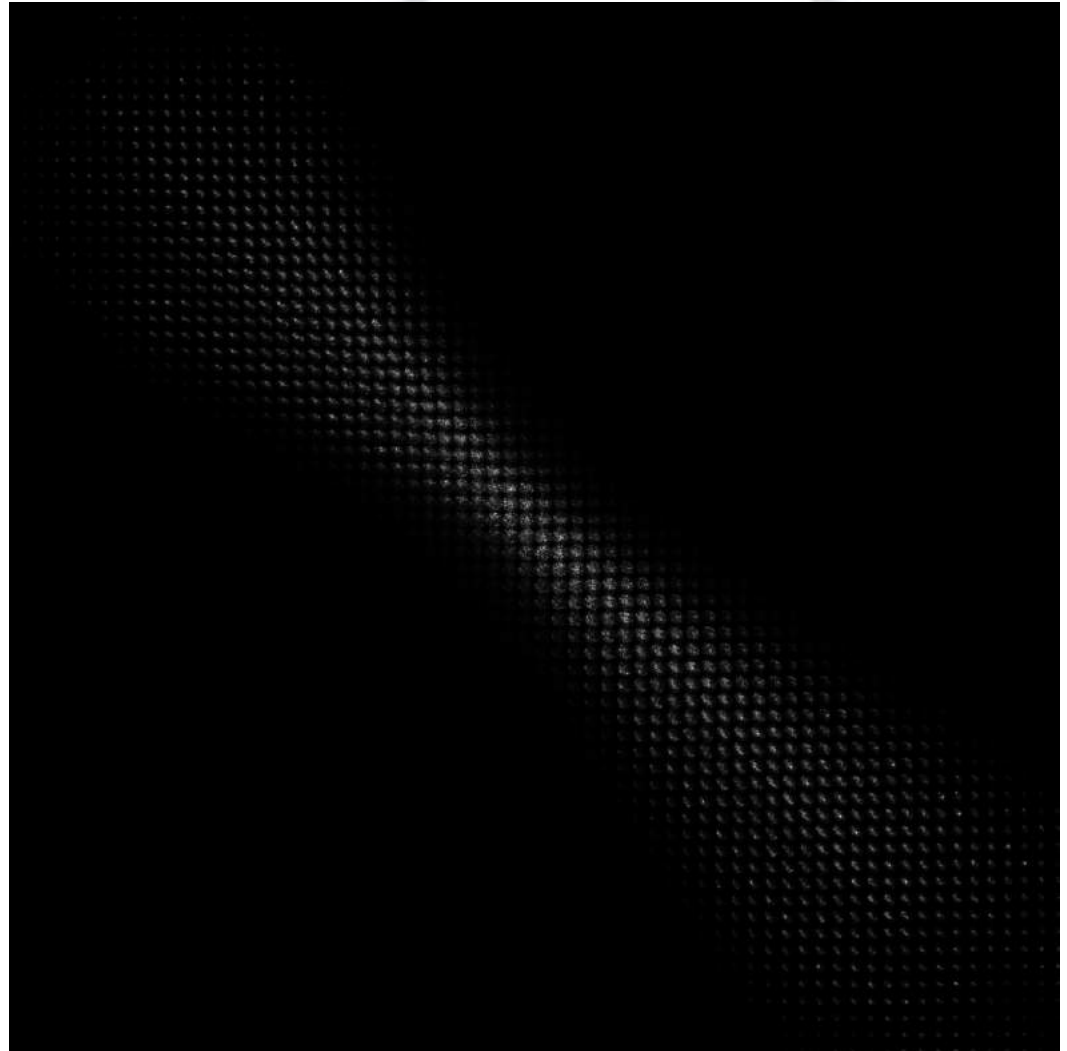


<http://www.ing.iac.es/PR/newsletter/news2/first.html>

- **LGS profile measurement**

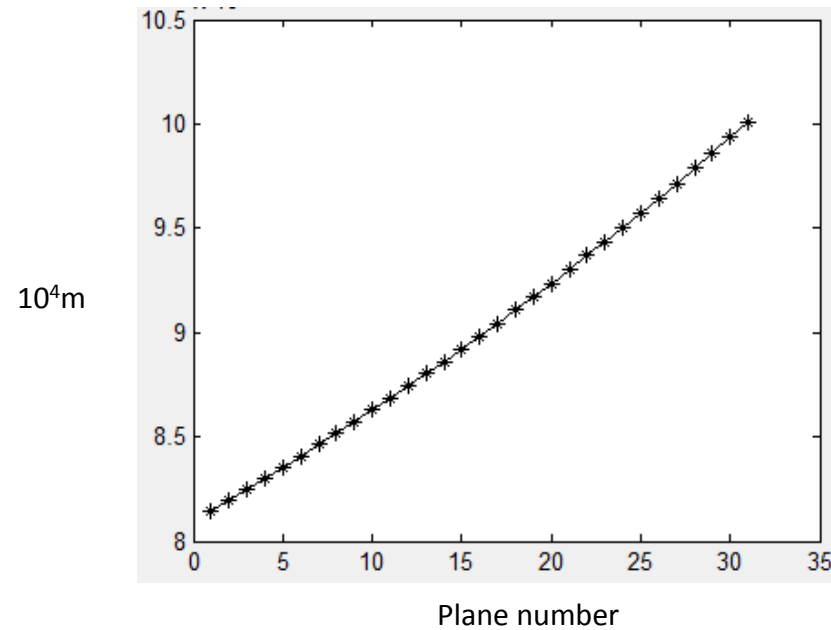
Simulation:

- 10m telescope
- F-number 1:17
- 16x16 px microlens
- Conjugate to 90km



- LGS profile measurement

Focal stack:



Linear distribution of planes



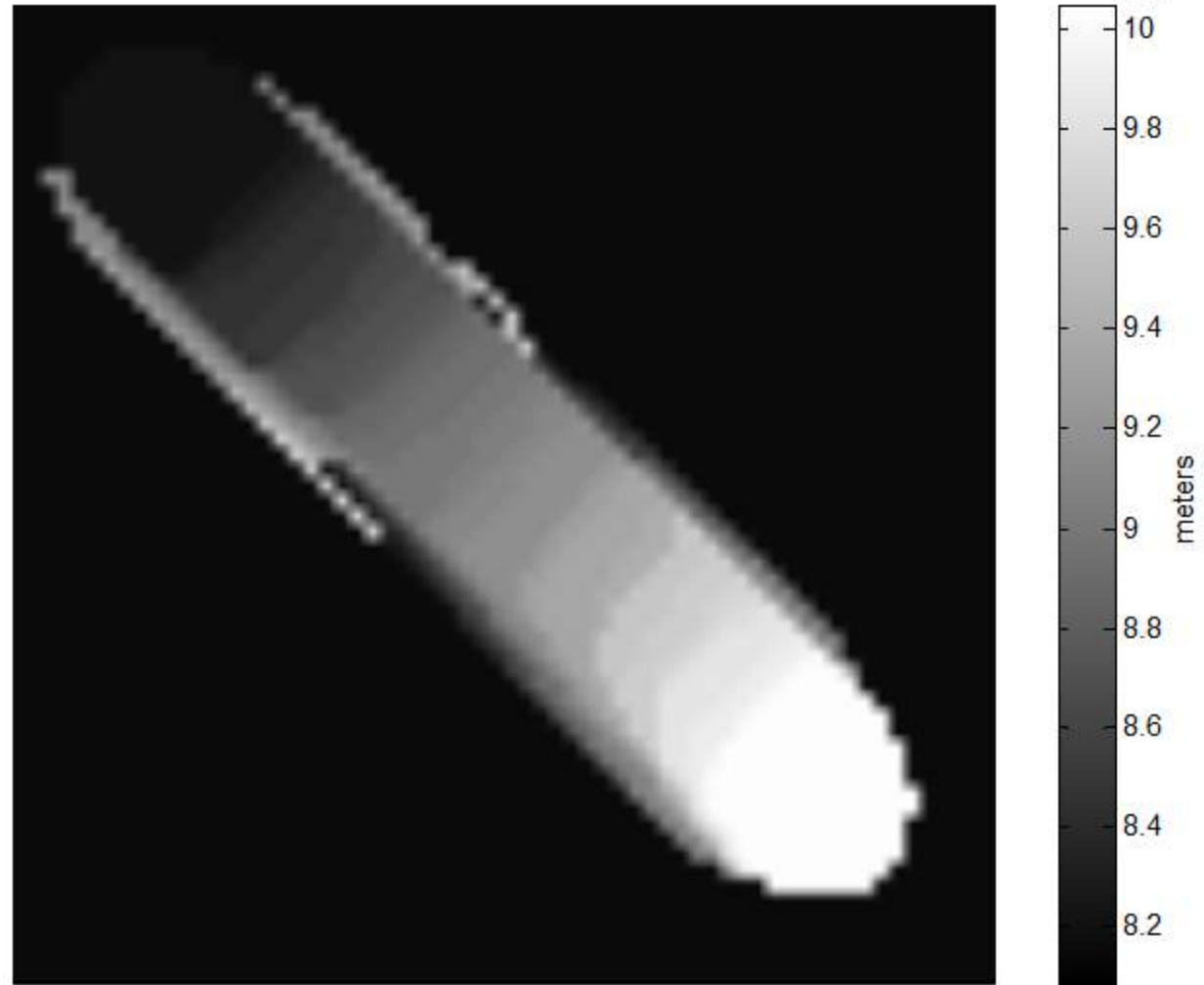
- LGS profile measurement



Depth map:

Mean resolution: 621.4 m

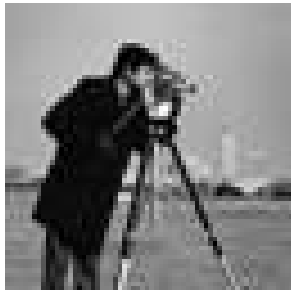
Number of planes depends
on the microlens resolution.



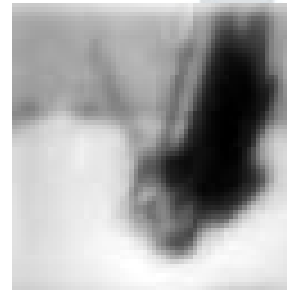
• Plenoptic deconvolution

- In the plenoptic sensor resolution depends on the number of microlenses.
- Deconvolution knowing only the plenoptic image and the optical design.

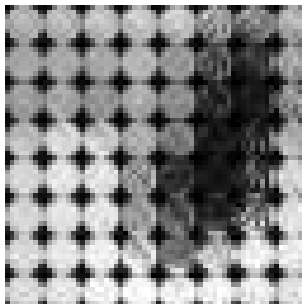
1. Object



2. Perturbation



3. Plenoptic image



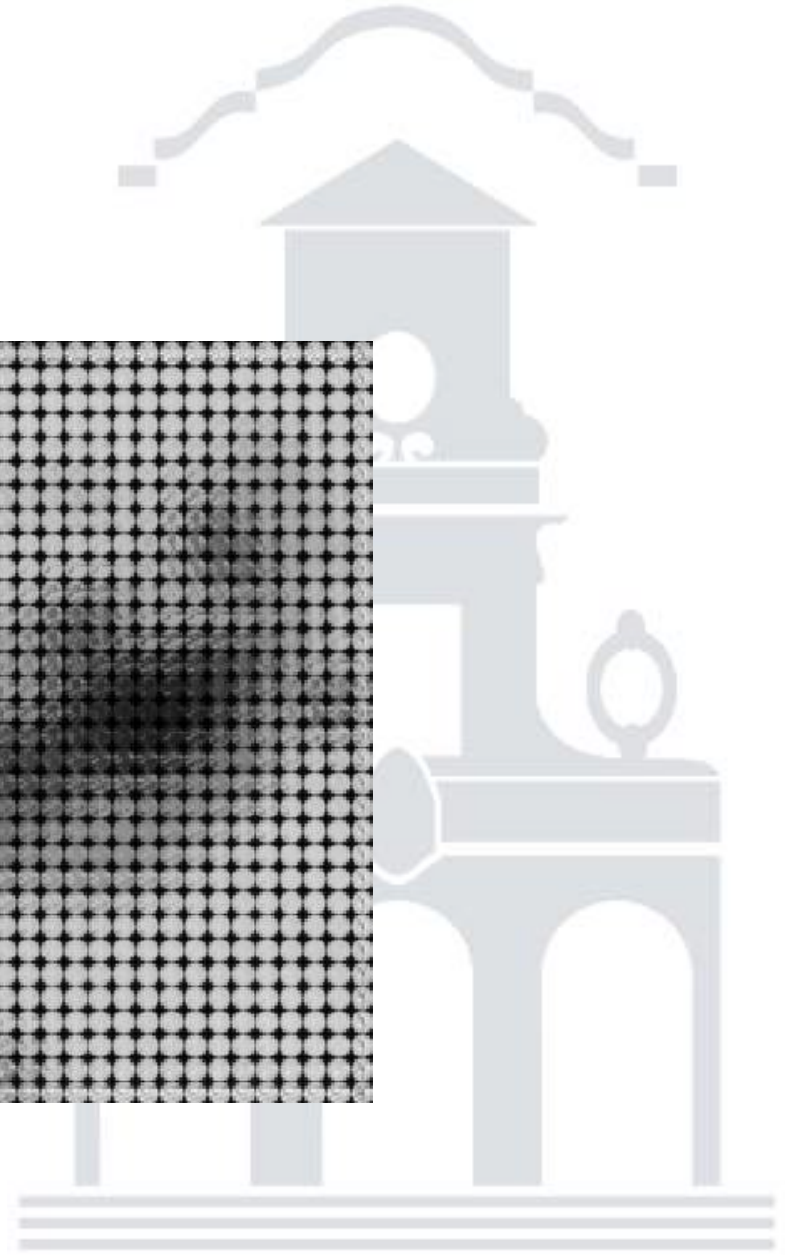
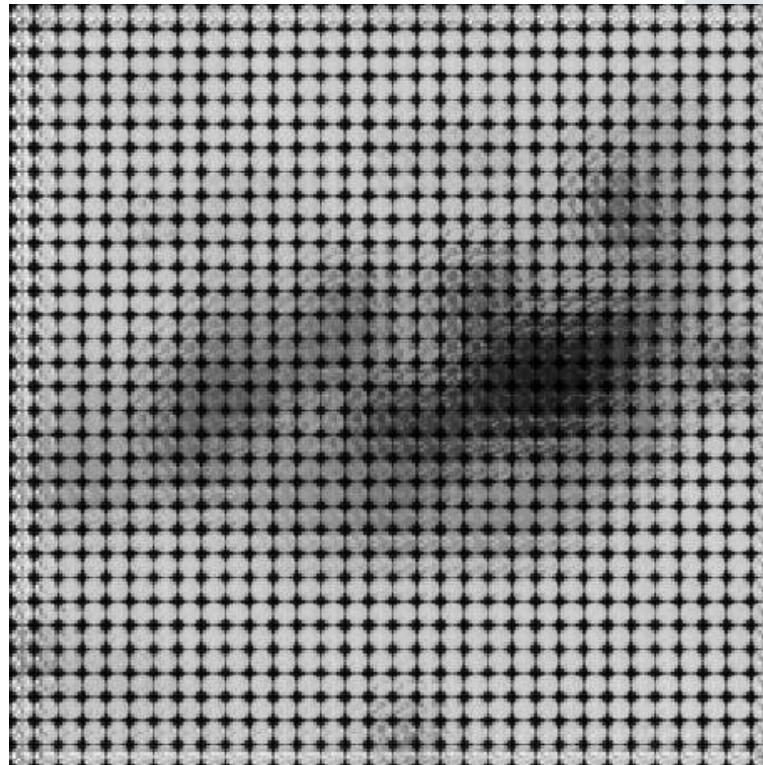
4. Recovered



Without perturbations and with full resolution

*Shroff, S. A., & Berkner, K. (2013). Image formation analysis and high resolution image reconstruction for plenoptic imaging systems. *Applied optics*, 52(10), D22-D31.

- **Plenoptic deconvolution**
 - **First step: Phase measurement**



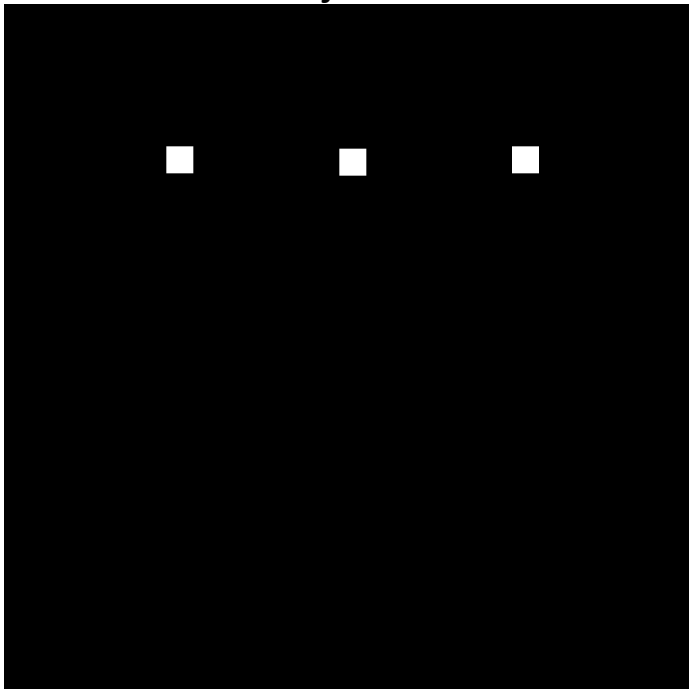
• Plenoptic deconvolution

- **Second step: Characterize the “Pupil impulse function”.**

For every point in the object there is an **unique impulse response** (PIF). Pupil impulse response is computed taking into account the phase.

$$I_{ulens}(x, y) = \mathcal{F}^{-1} \left\{ \mathcal{F} \{ U_1(x, y) e^{(-ik\theta)} \} e^{\left(-\frac{i}{4\pi} \lambda f (x^2 + y^2) \right)} \right\}$$

Object



Plenoptic image



- Plenoptic image can be written as:

$$[Iv_f] = [PIFv][Iv_o]^*$$

Where,

Iv_f , vector containing sensor data

Iv_o , object intensity

$PIFv$, matrix of stacked columns of impulse responses

*Shroff, S. A., & Berkner, K. (2013). Image formation analysis and high resolution image reconstruction for plenoptic imaging systems. *Applied optics*, 52(10), D22-D31.

- Solving the system:

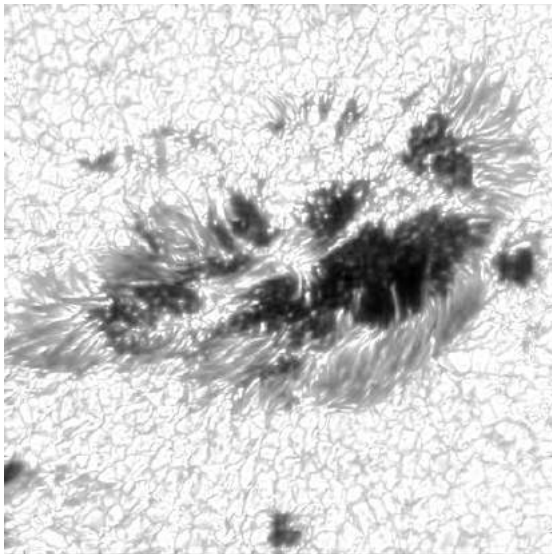
$$[Iv_o] = [PIFv]^{-1} [Iv_f]$$

Object intensity can be restored in original resolution

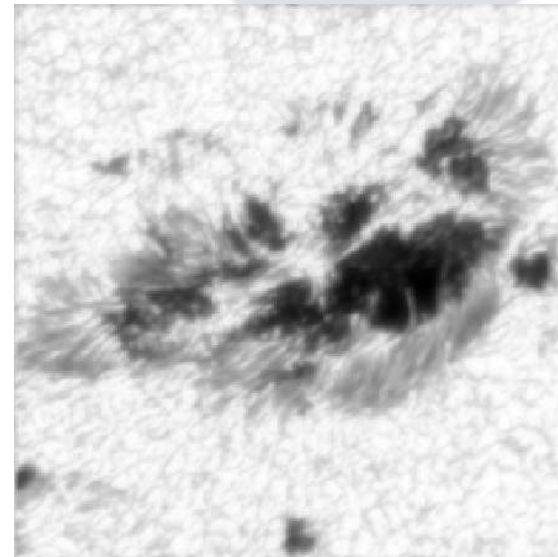
In absence of noise. System can be solved using the pseudoinverse of PIFv.

In presence of noise, an iterative least squares optimization works better

OBJECT



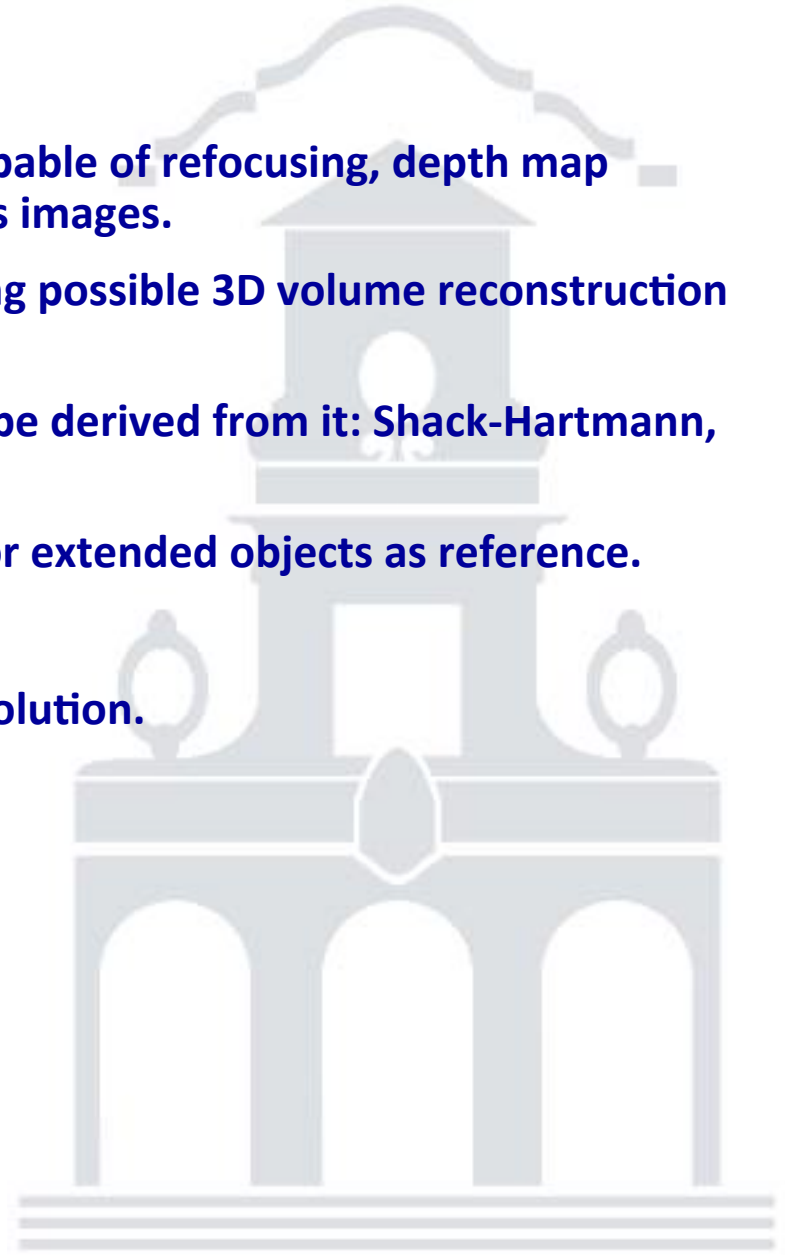
DECONVOLVED IMAGE



Loss of resolution is due to the wavefront phase used to generate PIF was estimated and not the real one.

Conclusions

- Plenoptic sensor as imaging sensor is capable of refocusing, depth map estimation and generation of all-in-focus images.
- It can be adapted to microscopes, making possible 3D volume reconstruction and refraction index tomography.
- As wavefront sensor, three sensors can be derived from it: Shack-Hartmann, curvature and pyramid.
- Tomographic capability using punctual or extended objects as reference.
- LGS profile measurement capability.
- Resolution can be recovered by deconvolution.



Acknowledgments

This work was partially funded by:

- National R&D Program (Project AYA2012-32079) of the Ministry of Economy and Competitiveness.
- European Regional Development Fund (ERDF)
- European Project FP7-REGPOT-2012-CT2012-31637-IMBRAIN
- University of La Laguna
- Instituto de Astrofísica de Canarias (IAC)



THANKS

For more information on the CAFADIS project visit:

www.cafadis.ull.es

